Technische Universiteit Delft

Sensor-Based Sorting of Post-Consumer Plastic Packaging

Analyzing False Calls of Near-Infrared Sensor Systems

N+P

TU Delft

Sensor-Based Sorting of Post-Consumer Plastic Packaging

Analyzing False Calls of Near-Infrared Sensor Systems

by

L.H. van Wolfswinkel

to obtain the degree of Master of Science

at the Delft University of Technology,

to be defended publicly on Friday January 14, 2022 at 10:00.

Student number:	4355202	
Project duration:	April 1, 2021 – January 14, 2022	
Thesis committee:	Prof. dr. P. C. Rem,	TU Delft, Chair
	Dr. M. C. M. Bakker,	TU Delft, daily supervisor
	Dr. M. W. N. Buxton,	TU Delft, supervisor
	Ir. K. Wierda MBA,	N+P Group (N+P)

An electronic version of this thesis is available at `http://repository.tudelft.nl/`.

TU Delft

Preface

Before you lies the final version of my master thesis which concludes my education at the TU Delft. The topic allowed me to combine my bachelor Mechanical Engineering, master Environmental Engineering and interest in sustainability. During the past nine moths I received a great deal of help at both the TU Delft and N+P in Rotterdam, where this research was conducted.

First, I would like to thank the graduation committee. My daily supervisor, Maarten, thank you for always being available when I needed help and coming to visit on site. Meetings of three hours long were the rule rather than the exception, which gave me time to gain a better understanding and discuss my doubts. Mike and Peter also joint the committee from the start, providing both written and oral feedback which contributed to this research. Thank you both for your input, time and expertise. Lastly, Klaas, thank you for asking the right questions which helped me reflect on my research approach along the way. Also the introduction to the design of experiments method and the related statistics (amongst others) was very educational. I also really appreciated the personal feedback throughout the process.

At N+P I also received a great deal of help. Thank you Naomi for helping me find my way around in the KSI and for answering all my questions (some even multiple times). I would also like to acknowledge the other colleges at N+P; Frans, Godfried, Ester, Helder, Patrick, Joost, Henk, Walter, Lindemar, Debby, Kamal, Mark, Tiest, Hayo and others working in the production for their involvement. Your enthusiasm, feedback, help while taking samples and walks during the break helped me a great deal and taught me more than just what was required for my thesis. As well as Kees and Monique who taught me a great deal about recognising different types of polymers. There was never a dull moment while sorting the samples in the cabin with you two, so thank you.

Next, I would also my family, friends and housemates. Of course my parents, for their care and support throughout my entire study and their efforts to improve the separation of waste at home. Max and Claire, I enjoyed these 4 months we spend together at the TU Delft. Especially studying together when everyone else was enjoying their weekends. Thank you to my housemates who were willing to listen, provide distraction, read a part of my thesis and prepare a meal even when I came home smelling a bit like garbage. Lilly, thanks for helping out with your design and UX skills. And last but not least, my boyfriend Pieter, who is currently working on his thesis as well, but was always prepared to help. Your structured way of working and attention to detail definitely improved my work. Your care and need for a good amount of sleep certainly improved my mood.

L.H. van Wolfswinkel
Delft, January 7, 2022

Abstract

Starting from the 1950s, plastic has found its way into many aspects of life; from packaging to transportation and construction. The annual global plastic production was estimated to be 330 million metric tons in 2017 and will be doubled within 20 years if the current growth rate persists. In Europe, packaging accounts for 40% of the annual plastic production. To decrease dependence on fossil fuels and the related emissions and reduce the negative impact of plastics that enter the environment, the EU targets to recycle 55% of plastic packaging material by 2025. A steady production of large quantities of high-grade plastic recyclate is essential to sell the recycled material on the market and substitute virgin plastics. But, achieving this high grade is difficult due to the wide range of polymers, including additives and fillers. This research focuses on the sorting step of post-consumer packaging waste in a Material Recovery Facility (MRF) that takes place before recycling.

In MRF's, Near-Infrared (NIR) sensor-based sorting systems are state of the art to create high-grade sorting products. NIR's use reflection spectra to identify and distinguish a range of materials including different types of polymers. The particles are fed to the NIR on a conveyor belt and are separated into two flows using actuators such as air nozzles. However, while sorting, False Calls (FC) occur when particles are incorrectly classified leading to a loss of valuable material or contamination of the product. Thus, this research aims to increase the understanding of false calls of NIR sensor systems, contributing to higher quality sorting products.

To reach this goal, possible causes of FC's and their dependencies on the feedrate, feed composition and feeding mechanism were identified. These causes were arranged into a framework consisting of six types of FC's. A distinction was made between errors that are working range related and those that are not. Particles outside the working range may be classified incorrectly even when fed in a monolayer and under perfect circumstances due to the properties of the particle.

The created framework was applied to a NIR in an MRF in the Netherlands which was tasked to separate non-plastic particles and PVC from plastic particles. Experiments were performed to single out the probability of each type of error to occur for 13 material classes. Next, the test results were implemented in a statistical model and a Monte Carlo simulation was performed. In this research, the varying input values were used to imitate the changing feed composition. Three scenarios of adjusted feed characteristics were analysed using the statistical model.

It was concluded that to optimize the sorting performance of the analysed NIR, all types of False Calls should be tackled. The feed of the analysed NIR contained a large share of particles outside the working range. So, even if the particles were to be fed in a monolayer the average grade of the product is expected to be around 85%. The combination of the experiments and the statistical model allows for an effective evaluation of the sorting performance and a clear indication of the most problematic aspects of the feed characteristics.

List of Figures

List of Tables

List of Abbreviations

DKR	Deutsche Gesellschaft für Kreislaufwirtschaft und Rohstoffe
DoE	Design of Experiments
FC	False Call
FCM	Food Contact Material
FP	False Positive
FPr	False Positive Rate
FN	False Negative
LOD	Laser Object Detection
MRF	Material Recovery Facility
NIR	Near-Infrared
PMD	Plastic verpakkingen, Metaal verpakkingen en Drinkpakken
PET	Polyethylene Terephthalate
PTF	Plastics To Fuel
TP	True Positive
TN	True Negative
UV	Ultraviolet

List of Symbols

Latin Symbols

$\dot{m}_{\text{feed}}$	Average input feedrate [kg/s]
F_1	Particle dimension (1) [cm]
F_2	Particle dimension (2) [cm]
G	Grade
k	Total number of runs
m	Mass
m_t	Total mass of particles targeted when sampling
m_{avg}	Average particle mass [kg]
N	Number of targeted particles
n	Number of particles
n_{FC}	Number of false calls per particle
N_{tot}	Total number of sampled particles
P	Probability of drawing targeted material class when sampling
p_{orient}	Probability of orientation error
$p_{\text{over,nst}}$	Probability of overlap error due to non-stationary agglomeration
$p_{\text{over,st}}$	Probability of overlap error due to stationary agglomeration
p_{rec}	Probability of recognition error
p_{mono}	Probability of false call when presented in a monolayer
p_{size}	Probability of size error
$p_{\text{syst,n}}$	Probability of causing a systemic error n times
p_{syst}	Probability of systemic error
p_{tot}	Total probability of false call
R	Recovery
R_{m}	Mass Recovery
F	DoE factor: MRF feed [%]
F_{max}	Maximum Feret diameter [mm]
F_{min}	Minimum Feret diameter [mm]
k	Number of factors DoE
N_{tot}	Total number particles in sample
R^2	Coefficient of determination
$\text{R}^2{}_{\text{adj}}$	Adjusted coefficient of determination
W	DoE factor: Opening of the windsifter blow valves [%]

Greek Symbols

α	Significance level
σ	Standard deviation
σ_{rel}	Relative standard deviation

Contents

1

Introduction

1.1. Background

Moving towards a circular economy for post-consumer plastic packaging waste has a wide range of advantages. Reducing, reusing, remanufacturing and recycling plastics lowers the negative environmental impact of (micro-)plastics on land and in the oceans (Jambeck et al., 2015) and decreases greenhouse gas emissions. The annual global plastic production was estimated to be 330 million metric tons in 2017 and will be doubled within 20 years if the current growth rate persists (Lebreton and Andrady, 2019). The expected growth and related emissions lead to an increasing consumption of the total carbon budget of 420–570 gigatons. The global carbon budget is an emission target set to keep the global warming below 2 degrees Celsius. It is estimated that by 2050 the accumulative greenhouse gas emissions of plastics from cradle to grave will take up 10% to 13% of this carbon budget (Shen et al., 2020). Only large efforts in the field of recycling, demand-management strategies and the application of renewable energy can compensate for the greenhouse gas emissions related to the expected growth of plastic demand (Zheng and Suh, 2019). Recycling plastics partly eliminates the first step of the linear chain, fossil fuel extraction, which is emission intensive (Shen et al., 2020).

Apart from the environmental benefits, the European Union mentions decreasing the dependence on fossil fuel as a reason to recycle plastics locally (European Commission, 2019). Finally, the current landfill of plastic waste and the leakage into the environment globally leads to lost economic potential. It is estimated that worldwide 95% of the value of plastic packaging is lost after the short term use due to the low collection rate and recycling rate (Ellen Macarthur Foundation, 2016).

In Europe, 39.6% of the produced plastic in 2019 was used for packaging of which only one third was recycled (Plastics Europe, 2020). More than paper and cardboard, plastic packaging increases the lifespan of food products and has a positive effect on food safety, thus refusing all plastic packaging may negatively affect other sustainability aspects like water usage due to an increase of food waste. The low weight of plastics makes it a more environmental-friendly option to transport than metal or glass (Andrady and Neal, 2009). Therefore, the EU has set the goal to recycle 55% of plastic packaging material in 2025 to tackle the problems related to plastic (European Commission, 2019).

However, to reach these recycling goals, multiple improvements in the plastic cycle have to be made. Hahladakis and Iacovidou (2018) claim that the technicalities, such as organisational barriers, lifestyle and the ability to properly recover materials lack behind the governance and new business models. To properly recover materials and maintain the value of plastics, closed-loop recycling is preferred

above down cycling in the circular economy framework (Ellen Macarthur Foundation, 2016). In practice, closed-loop recycling can only be achieved when the collected material has a high grade, like the deposit collection scheme for Polyethylene Terephthalate (PET) bottles. Adhesives, colorants and additives are used to optimize the mechanical and aesthetic properties of plastic to match their aimed purpose resulting in an enormous variety of plastics (Thiounn and Smith, 2020). The most suitable recycling method depends on the properties of the plastic. For example, melting of a batch of mixed plastic with different melting points affects the appearance and performance of the recycled product due to insufficient blending of the material (Hahladakis and Iacovidou, 2018).

So, to move towards a circular economy for consumer plastic packaging, high-grade sorting is essential. Therefore, this research will be focused on the recovery of plastics that takes place in a MRF. State of the art sorting facilities use a cascade of NIR sorting units to separate the incoming plastic packaging waste into multiple polymer types (Feil et al., 2019). NIR sensor sorting systems such as the system shown in Fig. 1.1 use the reflection of light beams to identify the material of the object and use actuators to separate the targeted materials from the material flow (Gundupalli et al., 2017).

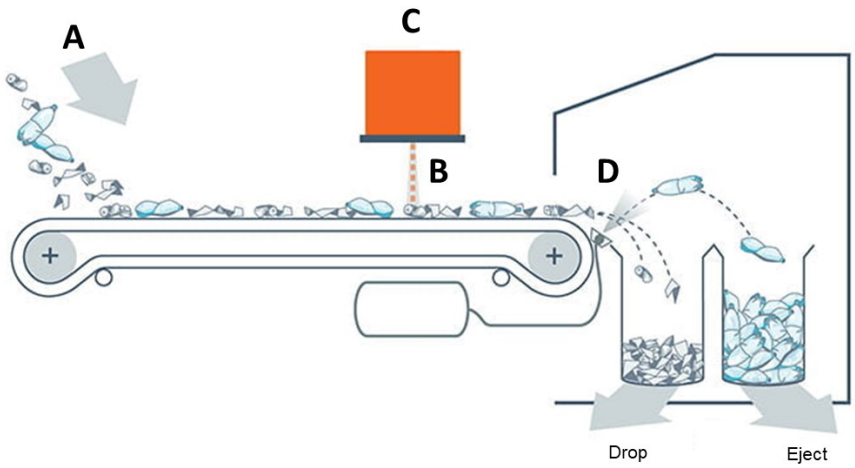

Figure 1.1: NIR sensor sorting system with conveyor belt consisting of a feeding mechanism (A), a light source (B), a processing unit (C) and a blowbar (D) (Tomra, 2021).

In practice, the NIR sensor sorting systems are not always used to their full potential (Feil et al., 2019). The performance is related to the number of times an object is not sorted into the correct material flow. Such an event will be referred to as a false call. Multiple factors reduce the performance of an NIR sensor: the feed, the NIR settings, the identification database, and level of regular maintenance, amongst others. The feed of a sensor can be characterised by three related variables. First is the material composition of the feed, this includes the material type, size, colour and shape of the particles. The feed composition also includes the amount of dirt on the surface of the particles. Second is the feedrate which is measured in mass, volume or particles per time unit. The final variable is the feeding mechanism which is the way the particles are placed on the belt. This, together with the material composition and feedrate leads to the occupancy rate and the overlap rate. In this research, the variables of the feed are referred to as the feed characteristics.

An NIR sensor system performs best when particles are fed in a monolayer with some space between the particles (Pascoe et al., 2010). Due to the heterogeneity of the input material, the individual sorting

units and the operational circumstances of an MRF, fluctuations in the feedrate and feed composition are known to occur (Curtis et al., 2021). The variations of the feed characteristics result in fluctuations in the occupancy rate and false calls. Controlling the feed characteristics can improve the performance of the sensor sorting system (Feil et al., 2019).

The influence of the feed characteristics on the sorting performance has been reviewed in previous research. The influence of the throughput rate, the share of targeted material, the roughness of material and the surface moisture have been analysed (Küppers et al., 2020)(Küppers et al., 2019)(Küppers et al., 2021). Also, a model was created with a predetermined probability of correct classification for common types of plastic packaging (Kleinhans et al., 2021). But the variables of the feed and the influence on the performance have not yet been set against each other and combined in one model. In addition, research performed on a lab scale is relevant for the understanding of the sorting performance. However, these experiments are not always able to capture the particle-to-particle interactions of heterogeneous waste. Khodier et al. (2021) states that real scale experiments are needed to transfer the results to applications in the industry. So, comparing the influences of the feed characteristics on the sorting performance of an NIR sensor sorting system in an industrial setting will point out the opportunities to optimize the feed to gain the desired quality results in an MRF. Currently, systems for smart control of flows in MRF's are being developed (Sarc et al., 2019). These systems aim to control the feedrate and feed characteristics by real-time adjustment of for example the shredder settings. The knowledge gained in this research about the optimal feed characteristics can also be applied to such smart systems.

1.2. Objective

The aim of this research is to increase the understanding of false calls of NIR sensor systems, contributing to higher quality sorted products that can open up the market of recycled plastics.

1.3. Research Questions and Scope

Based on the objective the following research questions are formulated:

Main research question:

To what extent do feedrate, feeding mechanisms and feed composition influence the type and number of false calls in sensor sorting systems and how can these false calls be reduced?

Sub research questions:

1. What is the working range of the sensor?
The working range of the sensor defines the ranges of the particle characteristics (particle size, shape, colour) that the sensor can process correctly with a high probability, given that the particles are fed under optimal conditions and in a monolayer. Knowing the requirements for the optimum input material allows to the correct evaluation of false calls.

2. What is the relation between each type of false call and feed characteristics (the average material composition, average feedrate and the feeding mechanism)?
The relation between the feed characteristics and false calls defines the NIR sorting performance. This information can be used to create a statistical model of the NIR sensor system.

3. What is the effect of short- and midterm fluctuations of the feed characteristics on the sorting performance?
Due to the input material of an MRF, the design of the sorting process and maintenance, variations in feedrate and feed composition may occur. These variations may influence the number of false calls. Studying the effect of the variations on the total amount of false calls may lead to more insight on the

acceptable ranges of fluctuations in the feedrate and composition.

Scope
Below the focus area and limitations of this research are summed up.

- The sorting performance of NIR sensor systems of post-consumer packaging waste in the Netherlands is analysed. The material is referred to as Plastic verpakkingen, Metaal verpakkingen en Drinkpakken (PMD).
- The research is conducted at an MRF in operation and not in a lab setting. Unforeseen alterations to the sorting system may occur but are monitored and noted.
- The settings of the sensor sorting system such as the splitter height, the air pressure of the nozzles and the classification algorithm will remain constant during the research.

1.4. Methodology

In this research, an experimental approach is used to analyse the influence of different types of FC's on the sorting performance of an NIR sensor system. The research is conducted at a Dutch MRF where PMD is sorted. An NIR sensor sorting system in the facility is chosen to build up and demonstrate the method. This NIR processes the most challenging feed in the MRF at the end of the sorting line. Due to the wide range of particle properties in the feed this NIR encounters all types of FC's. In Fig. 1.2 the experimental research methodology is visualised.

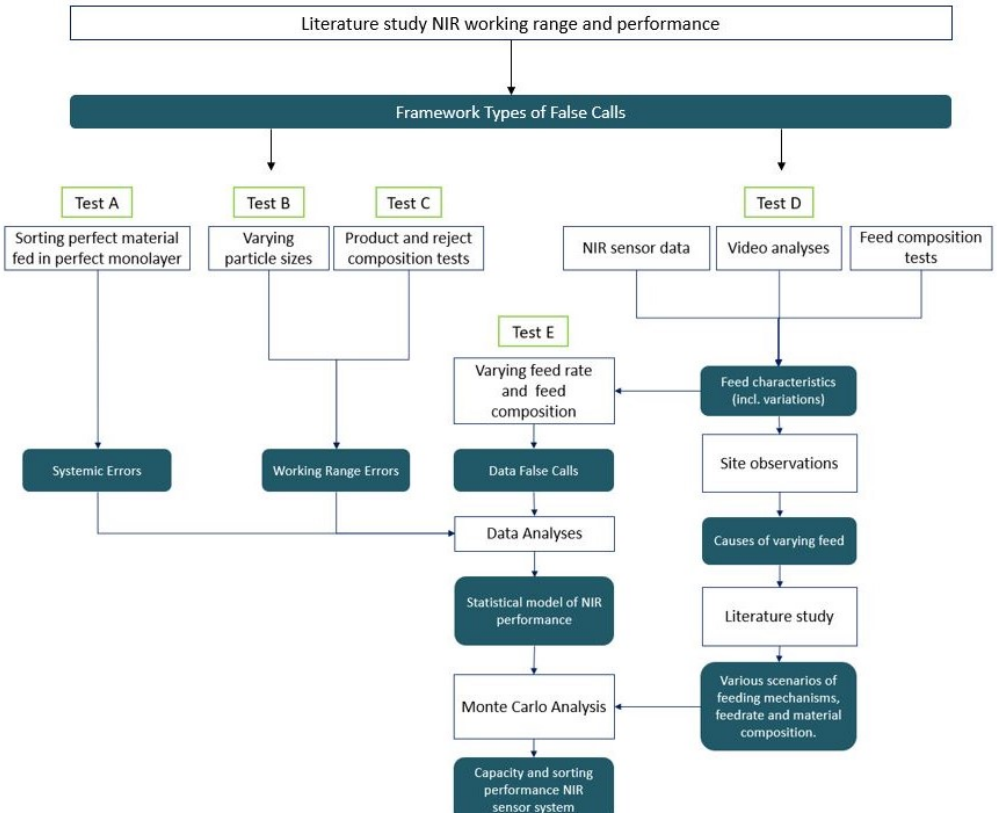

Figure 1.2: Research methods and corresponding tests. White blocks represent the research methods and blue the (intermediate) results and products.

First, types of FC's are defined and the feed characteristics that are expected to affect each type of false call are determined. Subsequently, the range of the feed characteristic of the chosen system is studied

using the data collected by the NIR system. Multiple tests will be conducted to isolate the influence of each type of FC. The feed characteristics will be varied using the Design of Experiments (DoE) method and the earlier found working ranges of the sensor. The performance is determined by analysing the samples of the material flows. In addition, a statistical model is developed to perform a Monte Carlo Simulation.

Key Takeaways Chapter 1

- High-grade sorting is essential to reach the recycling goals and move towards a circular economy for post-consumer plastic packaging.
- NIR sensor-based sorting systems are state of the art and are often applied to separate polymer types and increase the grade of products.
- A NIR makes False Calls while sorting which lead to a lower product grade or a loss of valuable material.
- In this research, a framework of types of False Calls is created, implemented on-site at a MRF and used to create a statistical model.

2

Theoretical Background

2.1. Post-Consumer Plastic Packaging

In The Netherlands, the average person creates 34,5 kg PMD waste per year of which 71% is collected separately (Milieu Centraal, 2018). Part of the remaining 29% is mechanically recovered from mixed household waste. In Table 2.1 the seven polymer types with the largest production share in plastic packaging in Europe are displayed (Plastics Europe, 2020).

Table 2.1: Most used polymer types of packaging material and common applications.

Polymer type	Abbreviation	Common packaging applications
Low Density Polyethylene	PE-LD	Bags for bread and frozen food, shrink wrap, container lids, squeezable bottles
High Density Polyethylene	PE-HD	Shampoo bottles, household cleaners bottles, juice bottles
Polypropylene	PP	Containers for yogurt and butter, bottle caps
Polystyrene	PS	Food service items, rigid food containers
Expanded Polystyrene	EPS	Take away food containers
Polyvinyl Chloride	PVC	Packaging of electronics and toothbrushes
Polyethylene Terephthalate	PET	Bottles for water and soft drinks, peanut butter jars

2.1.1. Polymer Waste Hierarchy

In 2008 the European Union created the Waste Framework Directive to set the definitions and basic concepts of waste management and unify the targets and the approach to tackle waste. The five-step waste hierarchy (Fig. 2.1), which is derived from the Ladder of Lansink, is the foundation of this framework. In the framework, recycling is defined as "any recovery operation by which waste materials are reprocessed into products, materials or substances whether for the original or other purposes.". It is specified that reprocessing materials into fuels, backfilling operations and energy recovery are not classified as recycling.

Recycling methods can be divided into upcycling and downcycling. In the case of upcycling, the product quality resembles the quality of virgin material. This is the most preferable option because the value of plastics is not lost and is applied mostly within the production process or for developed collection schemes like PET bottles (Al-Salem et al., 2009). Part of the collected and sorted plastics do not meet the quality standards required for upcycling. These mixed or contaminated plastics are treated and utilised in lower value plastic products like park benches, flowerpots and traffic signs. Chemical

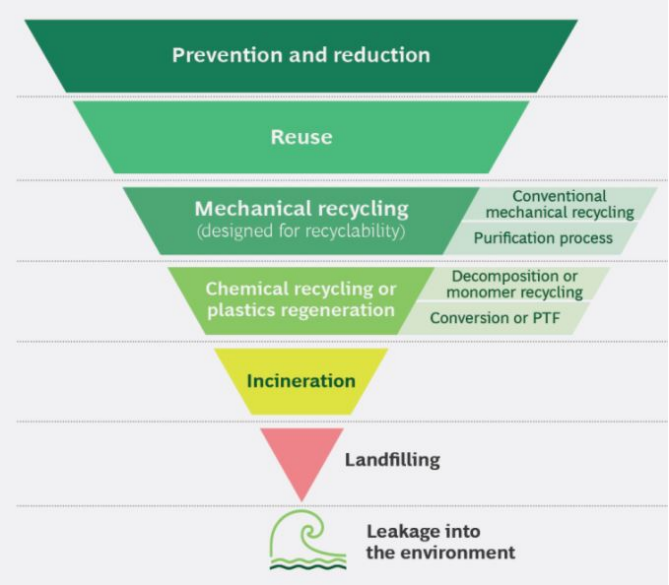

Figure 2.1: Plastic waste hierarchy (Rubel et al., 2019). Note: Chemical recycling does not comply with the definition of recycling as mentioned in the EU waste directive.

conversion or Plastics To Fuel (PTF) is often referred to as recycling but does not comply with the definition of recycling in the European Waste Directive (2019). Energy recovery by combustion of plastics is applied when the before mentioned methods are not possible due to e.g. economical restrictions.

Recycling is challenging due to the wide range of types of plastics and additives and fillers. Fillers such as calcium carbonate and talc can increase hardness and is an inexpensive way to increase the bulk of the plastics (Ügdüler et al., 2020). Additives are added to the plastic packaging to make them fit for purpose by for example increasing the tensile strength, protecting against Ultraviolet (UV) light or decreasing flammability. However, these additives may decrease the recyclability and may lead to health risks during recycling or environmental impact when plastics disintegrate after littering (Hahladakis et al., 2018). Also, laminated plastic packaging consisting of multiple polymer types will always be downgraded due to the low grade of the product (Shen and Worrell, 2014). Finally, polymers will degrade over time due to external factors such as UV. Therefore, a closed-loop in which no plastics are downcycled currently appears unattainable.

2.2. Recycled Polymer Market

A study of the Dutch recycling system for post-consumer plastic packaging waste in 2017 states that a large fraction of the recycled polymers is not suited for high-end consumer goods markets like food packaging and household appliances (Brouwer et al, 2019). For safety reasons, Food Contact Material (FCM) has to comply with strict regulations. Not only does FCM have to meet contamination and migration limits, the maximum quantity of a substance that is allowed to migrate from the packaging into food, but also full traceability throughout the plastic chain and separation of FCM and Non-FCM are required (De Tandt et al., 2021). The latter two requirements pose a technological challenge to processors and recyclers of post-consumer plastic waste. It is estimated that in Europe, 5% of the food packaging is recycled and used to produce food packaging again (De Tandt et al., 2021).

On the other hand, there is a lack of international certification for recycled plastics per product group (De Tandt et al., 2021) (Shamsuyeva and Endres, 2021). Quality not only depends on the share of contamination but als on the type of contamination. At present, quality concerns and the low prices

of high-quality virgin plastics keep packaging producers from using recycled plastics (McKinnon et al., 2018). Also, producers require a steady, large volume flow with the security of supply.

So, the loop of plastic food packaging is hard to close. In addition, the limited uses for low-grade recycled polymers and the low oil prices keep the market value low (Brouwer et al., 2020). Recycled polymers with high purity can make the use of recycled plastics more attractive for manufacturers and contribute to a circular economy (Rem, 2017) (Luijsterburg and Goossens, 2014).

2.2.1. Quality

In The Netherlands, municipalities are responsible for the collection and recycling of PMD. The municipalities or the recyclers receive a compensation from the packaging industry to outsource the different steps of the chain. The quantity and quality of the material throughout the chain is monitored by Nedvang, a company founded by the packaging industry, using the Deutsche Gesellschaft für Kreislaufwirtschaft und Rohstoffe (DKR) specifications. These specifications set quality targets for the five types of products that are produced: PET (DKR328-1), PP (DKR324), PE (DKR329), foils (DKR310) and mixed plastics (DKR350). These criteria determine the financial compensation for the organisations involved in the chain but can be requested by the purchasers too(Ooms et al., 2010).

The Mixed plastic product mainly consists of PE and PP. A limit is set for the share of PVC. PVC is undesirable because it releases toxic gasses when heated or dissolved and decreases the quality of the recycled product due to the formation of compounds Park et al. (2007).

2.3. Polymer Sorting

2.3.1. State of the Art

Mechanical waste processing plants usually apply the following steps: comminution (using e.g. shredder or bag opener) to liberate particles and reduce the size of large outliers (Julius and Pretz, 2012). Then, size classification to separate the waste streams into flows with a particle distribution suitable for the following treatment steps. And lastly, the separation is based on a combination of properties that are unique for a material group like magnetic properties, material type, density or shape (Feil et al., 2016).

2.3.2. Optical Sorting

Optical sorting was originally developed for the food industry. An optical sorter uses a combination of a light source and a sensor to identify the shape, colour or chemical composition of a particle. Based on classification criteria, the particle is identified as targeted or non-targeted material and processed accordingly by a set of actuators. This non-destructive inspection method has a short measuring time which makes it very popular to sort material at a high throughput rate (Zerbini, 2006). In the food industry the particle characteristics of the feed like grains, nuts and fruit, are very uniform. This enables monolayer feeding and contributed to the success of optical sorting in this industry. The application extended to the mining industry and pharmaceutical industry and was first applied to process recyclable material in the waste industry around 1990 (Julius and Pretz, 2012). An optical sorting system generally consists of four components; the feeding mechanism, the light source, a digital processing unit and actuators (Fig. 1.1). Depending on the application and budget a spectrum is chosen (Rozenstein et al., 2017).

2.4. NIR Sensor Sorting Systems

2.4.1. Working Principles

NIR sensor-based sorting units use reflection spectroscopy to identify materials. A light beam including wavelengths in the near-infrared spectrum (750 to 2100 nm) is emitted towards the conveyor belt. The intensity of the reflection and absorption of wavelengths in the spectrum depends on the chemical and physical properties of a material, like the molecular composition and surface conditions (Küppers et al., 2019). The materials can be distinguished by the peaks in the reflection spectra (Fig. 2.2). Black or dark materials absorb more light and are therefore less visible and can not be classified correctly. The absorption spectrum of specific wavelength ranges can be influenced by surface moisture (Küppers et al., 2019). Higher surface roughness of the particles, on the contrary, increases the amount of raw data and improves the classification because of less background noise (Küppers et al., 2019). The refection of the light beam is collected from spatial areas on the particle surface called pixels. The spectrum is evaluated for each pixel. The size of the pixel, together with the belt velocity and the frame rate leads to the minimum particle size that can be classified correctly. For example, the NIR analysed in this research has a pixel size of 8 mm. In the industry, chemometric methods are used to interpret

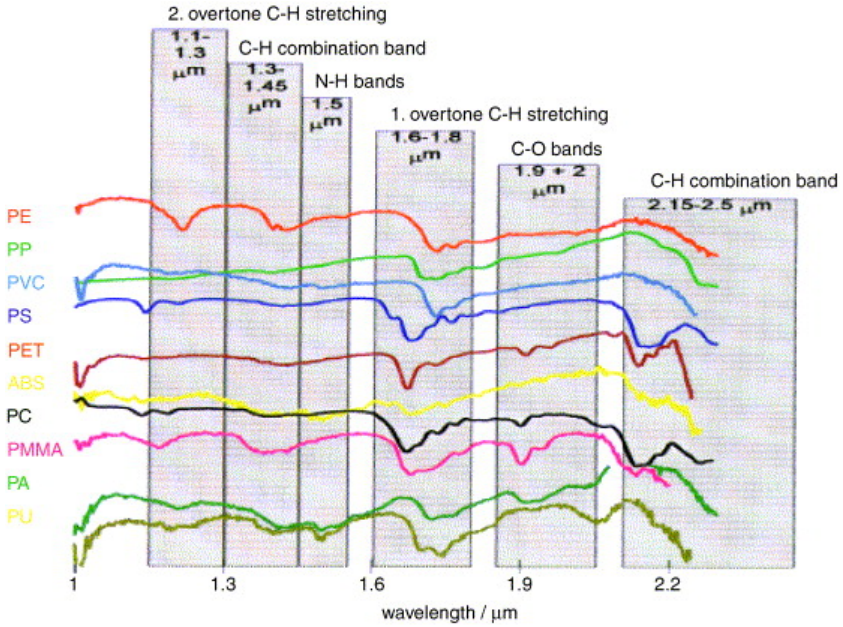

Figure 2.2: Spectra for commonly used plastic packaging materials (Tatzer et al., 2005).

the optical data (Tatzer et al., 2005). Collected data of spectral bands of known material classes are uploaded to the data processing system as a reference database. During sorting, the incoming data is compared to the database and the materials are identified. This method requires updates when the feed composition changes or if new classes of materials are added.

Once the material is identified based on the reflection spectrum, a signal is sent to the connected actuator to eject the material or not. Some data processing systems offer the option to process the acquired data to influence the selectivity of the sensor. For example, if a high recovery of PET is aimed, one can increase the 'weight' of all PET indicating pixels and thereby change the surrounding pixels to favour a "PET" identification. This will affect the action of the actuator and decrease the chance of incorrect sorting of a valuable material like PET. By doing so, more non-PET materials may be ignored by the NIR and therefore move along with the PET, decreasing the purity.

In case air valves are used as actuators, the time frame of the activation depends on the number of

pixels recognised and the belt velocity. In some systems, the time frame can be adjusted manually. The trajectory of the particle is affected by its shape, density, moment of inertia, air nozzle size, airflow and the distance between the air nozzles. After correct recognition of the material by the sensor, a heavy particle might still be discharged incorrectly i.e. dropped due to insufficient applied air pressure from the valves.

2.4.2. The Working Range

The working principles of an NIR result in the working range. This is a range of particle characteristics to which the material has to comply to have the highest probability to be sorted correctly apart from being fed in a monolayer. The following particle properties play a role in the working range:

- Minimum particle size: Number of correctly identified pixels that is required to activate the actuator may not be met.
- Maximum particle size: Can be too heavy to move over the splitter or may get stuck.
- Materials characterised and sorted in a database: The reflection spectrum is not recognised.
- No black/dark materials: Little light is reflected in the NIR spectral region preventing correct identification (Rozenstein et al., 2017).
- Surface conditions (maximum amount of surface moisture, dirt or grease).
- Folded particles and complex shapes: Bended surfaces may lead to overexposure due to the high reflection of light (Chen et al., 2021).
- Particles that tend to roll or float: The timing of the activation of the actuator is based on the belt speed. Relative moment to the belt may lead to arriving to late or too early to be ejected.
- Minimum and maximum density: Particles may be to heavy to move over the splitter. Light materials may flutter into the wrong section after ejection.

2.4.3. Feed Characteristics

As mentioned in the introduction, the NIR feed passing the sensor scanline can be described by three related variables: the feed composition, the feedrate and the feeding mechanism. Combined, they describe the occupancy rate and overlap rate on the conveyor belt.

feedrate: The feedrate, also referred to as the throughput, can be defined using the mass rate ($\dot{m}_{\text{feed}}$) [kg/s] or the particle rate [nr/s]. Since plastic packaging has a relatively low density, in research the particle rate is applied. In the industry mass rate is more common. Average particle mass can be used to calculate the mass feedrate if particles have about the same size. In the industry, plant operators have to balance between product value and technical limitations when controlling the input of a facility (Feil et al., 2017).

Occupancy Rate: The occupancy rate [%] is the share of the sensor detectable zone of the belt that is covered with particles. The occupancy rate can be defined as an average over the belt width per second or specified at intervals along the width. Küppers et al. (2019) argue that the capacity of an NIR sensor system should be indicated using the occupancy rate instead of the feedrate as the occupancy rate and the related overlap rate are directly related to the sensor performance.

Agglomeration and Segregation: In the heterogeneous waste flow, interaction between particles or between machine parts and particles may occur. Due to shape, adhesion or gravity, multiple objects may act like one, which is referred to as agglomeration. Segregation occurs when objects with similar attributes group in the process, causing an inhomogeneous flow for specific particle properties such as size or shape.

2.5. False Calls

The NIR sensor sorting system is a binary classification system; the incoming material is sorted into two classes based on a classification rule. In the case of polymer sorting, the feed is sorted into a product fraction, which contains the most valuable material, and the residue. The sensor system can be programmed to eject either the product or the residue, respectively called positive and negative sensor sorting. The choice for either option depends on the share of valuable material and contamination. While sorting, errors may occur and valuable material is lost in the residual fraction or the product fraction is contaminated. When a non-targeted particle is ejected, it is known as a False Positive (FP). When a particle is not ejected when it had to, it is called a False Negative (FN). The fractions often are non-symmetric meaning that the chance of a FN is different from the chance of a FP (Ooms et al., 2010). Together, these errors are referred to as False Calls. Correctly processed particles are True Positive (TP) when ejected or True Negative (TN) when not ejected. Fig. 2.3 displays the four outcomes of a binary classification system for both positive and negative sorting.

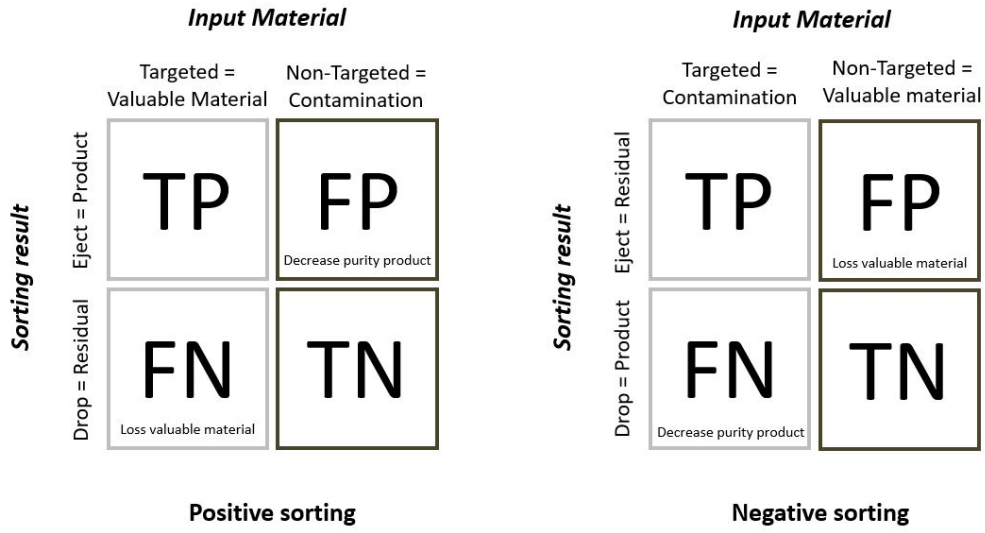

Figure 2.3: Contingency table: False Calls of positive and negative sensor sorting.

To sum up:

Total targeted material = Material to be ejected = P = TP + FN
Total non-targeted material = Material to be dropped = N = TN + FP
Total feed = targeted material + non-targeted material = P + N

Drop fraction = TN + FN
Eject fraction = TP + FP

2.5.1. Performance

The sorting performance of this binary classification system can be described departing from the number of particles (n) [nr/s] or using the mass (m) [kg/s]. The former is useful to analyse the performance in detail by looking at the behaviour of individual particles and to create a statistical model. The latter can be applied to describe the sorting results of a NIR and is applied in the industry. Next, both approaches will be described starting with the particles.

The terms introduced in Section 2.5 can be used to describe the share of particles that is sorted correctly. The fraction of targeted particles in the feed that ends up in the drop fraction can be expressed as the False Positive Rate (FPr)(Eq. 2.1a). Correspondingly, the **FNr!** (**FNr!**) is the share of non-targeted material that is incorrectly ejected (Eq. 2.1b). This approach is applied by Gülcan (2020) in the mining industry and Bukovec et al. (2007) in the pharmaceutical industry. In the case of negative sorting, a low FPr would mean that a large fraction of the contamination is removed from the valuable material. If the FPr is high, it would imply that a lot of valuable material is lost in the residue. So, a low FPr and FPr are beneficial.

$$\mathrm{FNr} = \frac{FN}{P} \tag{2.1a}$$

$$\mathrm{FPr} = \frac{FP}{N} \tag{2.1b}$$

In the industry and partly in research, the performance indicators are based on mass. The plant sorting performance is judged on the grade (G), the recovery (R) and the mass recovery (R_m) of the valuable materials. The grade, also referred to as the purity, is the percentage of valuable material in the product (Eq. 2.2a). The recovery represents the amount of valuable material from the feed in the product and is determined by the TPr and the average particle mass (m_avg [kg]) (Eq. 2.2b). The mass recovery can be used to quantify the product in relation to the feed (Eq. 2.2c). In this research, discharge (D) is added to the performance. This performance indicator describes the share of non-valuable material that is removed from the feed and does not end up in the product. These performance indicators are also applied in earlier research by Küppers et al. (2020).

$$G = \frac{\text{Valuable material in product}}{\text{Total product}} \tag{2.2a}$$

$$R = \mathrm{TPr} * m_\mathrm{avg} = \frac{\text{Valuable material in product fraction}}{\text{Valuable material in feed}} \tag{2.2b}$$

$$R_\mathrm{m} = \frac{\text{Product}}{\text{Total feed}} \tag{2.2c}$$

$$R_\mathrm{m} = \frac{\text{Non-valuable material in residue}}{\text{Non-valuable material in feed}} \tag{2.2d}$$

Depending on the position of the sorting system in the process line, the product and residue of the sensor system are sorted further using additional steps down the line.

2.5.2. Causes of False Calls

In literature, multiple parameters that influence the performance of NIR sensor systems are identified. To get a grip on how the complex and interrelated factors affect the sorting performance, the parameters have previously been grouped. Küppers et al. (2020) organises the parameters into two groups based on the cause of the failure of the sensor: identification errors and discharge errors. The first is for example influenced by surface moisture and the latter by share of targeted material. However,

variables like throughput influence both errors. In another approach, Gülcan (2020) divides them into geometric parameters (classification algorithm, the position of the splitter, feeding mechanism, etc.) and the process parameters (throughput, share of targeted material, size distribution, etc.). Other papers sum up a few causes of incorrect classification such as the inability to detect black or contaminated material and the sub-optimal material flows due to preceding process steps (Feil et al., 2019).

In this research, the errors are divided into six categories of false calls. These categories represent the underlying causes of the underperformance of the sensor system. This approach assumes the settings of the NIR, the geometric parameters, are constant. In Fig. 2.4 an overview is presented of which the framework is based on the lectures of Bakker (2020). First, the working range errors will be clarified.

Working Range False Calls

Working range errors occur when a particle is not suited for the used NIR system. This means that if the particle is fed in a monolayer under perfect circumstances, the particle will still not be correctly recognized by the sensor or ejected by the actuator. Working range false calls can be avoided by preprocessing or corrected by additional separation steps using a different separation principle or an NIR which classification algorithm is trained using another adapted teach and learn set.

Orientation: The characteristics of the particle may lead to an unfavourable orientation on the belt. An orientation is unfavourable if for example the dirty side or label is facing upwards and the material can therefore not be identified correctly by the classification algorithm. Also, a round shape or asymmetrical density of the particle may prevent it from lying still on the belt. The particle is therefore not recognized correctly by the NIR sensor, does not reach the actuator at the predicted time, or is placed in a way that influences the trajectory when ejected and thus failing to be thrown over the splitter. Orientation errors may be deterministic, for example when a particle is too heavy to be thrown over the splitter no matter the orientation, or if all sides of the particle are covered in dirt.

Size: Every NIR has a minimum and maximum particle size which is recommended by the manufacturer. Particles below the specified size may not be classified and ejected correctly. Above this minimum value, however, particles may still encounter difficulties due to size. The chance of correct sorting increases fast with particle size until size no longer plays a role.

Recognition: Targeted materials that do not have the targeted attributes are incorrectly sorted. For example when a particle consists of a combination of recycled PE and PP which does not occur in the database of the NIR sensor and is therefore not recognized as targeted material. The same goes for non-targeted material that happens to have certain undesired targeted attributes, like medical objects that are made of plastics but are not allowed in the plastic product. Finally, black materials might not reflect enough light to be classified correctly.

False Calls Unrelated to Working Range

Some stochastic errors can happen to all particles in the feed. The feed characteristics influence the probability of these stochastic errors. When a batch of material is sorted multiple times under the same process conditions, the share of these stochastic errors can remain constant, but the particles involved will differ. However, some particles may be more likely to be involved in this stochastic error than others.

Monolayer Overlaps: Particles may overlap on the belt due to the feeding mechanism and the feedrate or agglomeration. Overlapping may lead to incorrect identification of (part of) the materials involved. If a particle is correctly identified but is placed too close to an adjacent particle, it may be co-deflected (Pascoe et al., 2010). The particle characteristics influence the chance of overlap. Long and thin particles with a high shape factor increase the chance of overlapping (Wen et al., 2021). Also,

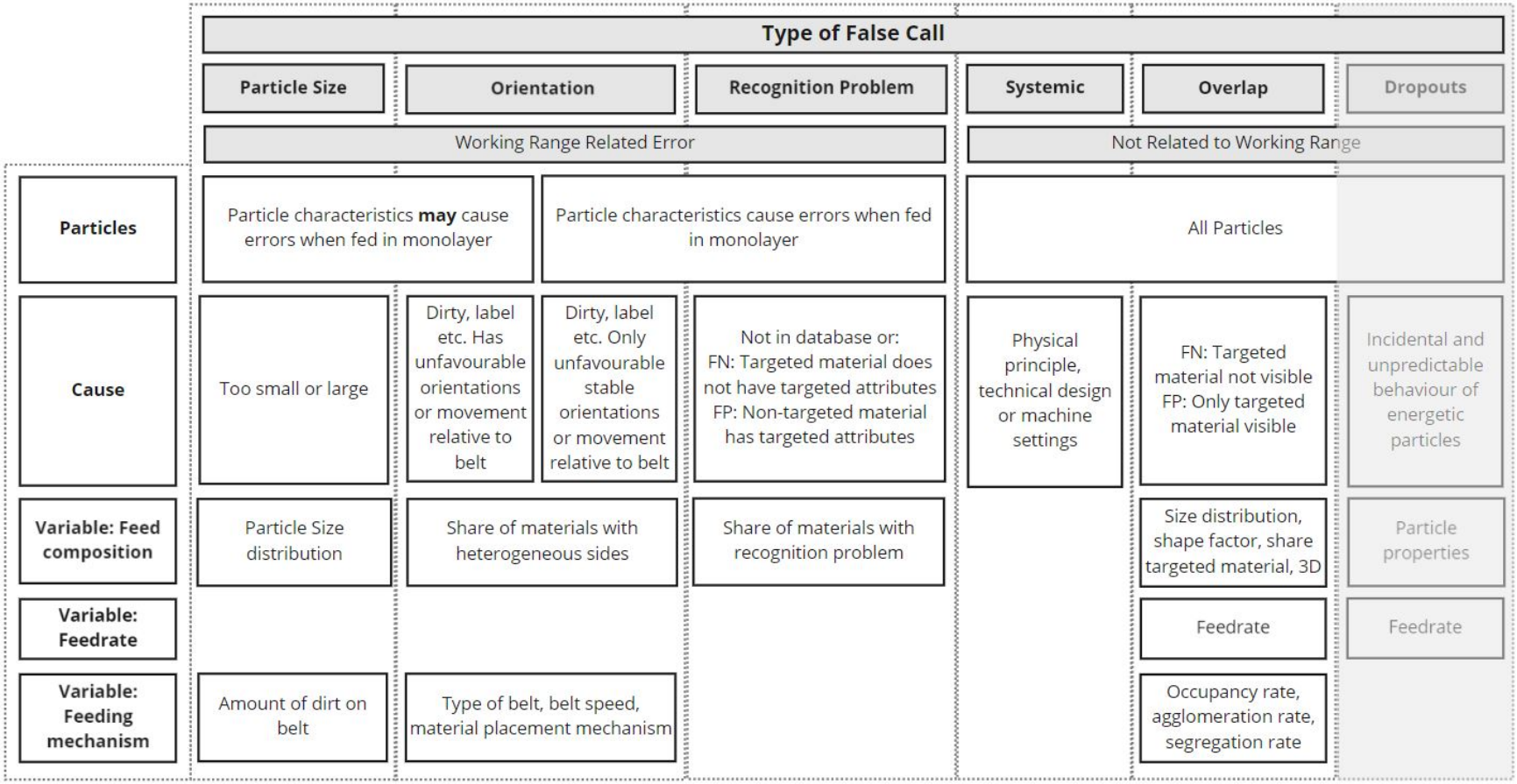

Figure 2.4: False Call framework including the dependency per type of error on the feed characteristics. Based on lectures of Bakker (2020).

when a particle has a 3D shape, it is less likely to be involved in overlapping due to its ability to roll when dropped onto the belt. The chance of an overlap leading to a false call depends on the share of targeted material because it influences the chance the overlap leads to an unwanted permutation (i.e. FP or FN). To minimise the chance of overlap it is recommended to narrow the size distribution as much as possible (Wotruba, 2006) (Julius and Pretz, 2012). Due to preceding collection and sorting steps, some particles form agglomerated groups. The agglomeration of particles inhibits monolayer feeding. Therefore it is considered a cause of overlap errors in this research.

Systemic: A sensor system may cause errors due to for example the physical design or principle shortcomings of the system. These errors are independent of the particle characteristics. Even if the material is within the working range and is fed in a monolayer, systemic errors may occur.

Dropouts: In the sorting system, unexpected errors may occur due to the energy of particles. For example, when two particles meet in a mid-air collision after ejection by the blow valves. It is expected that the chance of a dropout increases with the feedrate. However, since sensor systems should be fed in an organised monolayer the chance of a dropout is assumed to be negligible.

In the experimental part of this research, the probability of each type of FC will be determined. An overview of the FC's and the assigned symbols is given in Table 2.2.

Table 2.2: Types of FC's and assigned symbols of the probability.

Type of False Call	**Symbol**	**Outcome (FP, FN)**
Systemic	p_{syst}	Both
Size	p_{size}	FN
Recognition	p_{rec}	Both
Orientation	p_{orient}	Both
Overlap: Monolayer	p_{over}	Both
Overlap: Stationary Agglomerate	$p_{\text{over,st}}$	Both
Overlap: Non-stationary Agglomerate	$p_{\text{over,nst}}$	FN

2.5.3. Relation Between Feed Characteristics and Sorting Performance

The influence of feed characteristics on the sorting performance of optical sorters has been investigated in literature. The research is focused on the mining industry and waste industry since these industries encounter trouble with the heterogeneous feed. The sensor type, settings and classifying system differ in each research. In addition, the type of sorted material differs as optical sorters are applied in different industries. Therefore, the exact values found in previous research can not one-to-one be applied to other sorting systems, but general relations can be established. Here, the findings are summed up per industry and per type of optical sorter.

Mining Industry
VIS optical sorter

- For a constant particle size distribution, an increase of feedrate leads to a decrease in sorting efficiency (Gülcan and Gülsoy, 2017). This is mainly due to the ejection of non-targeted particles when particles are too close to each other. A decrease in feedrate may lead to an improved distribution of particles on the belt because of fewer particle interactions preventing movement across the belt (Pascoe et al., 2010).
- At a steady throughput, sorting performance decreases as particle size decreases. It is suggested that the reduced performance is due to the perception capacity of the sensor and the accuracy of the nozzles (Gülcan and Gülsoy, 2017) (Pascoe et al., 2010).

- An increase in the share of material to be ejected causes a decrease in sensor sorting efficiency. This is likely due to an increase of the probability that two overlapping particles are a combination of targeted and non-targeted material (Pascoe et al., 2010).

Waste Industry
NIR optical sorter

- A higher feedrate decreases the grade, recovery and mass recovery of the product (Küppers et al., 2020).
- The share of eject material in the feed influences the incorrectly discharged particles: the FPr is relatively highest around 50 percent, and quantitatively around one-third (Küppers et al., 2021).
- Yield is not affected by the share eject material for plastic squares in the range of 45 to 55 mm (Küppers et al., 2021). However, the share of eject materials did influence the yield for larger rectangular material (Küppers et al., 2020). It is hypothesized that the influence of the share of eject particles further depends on the size distribution and the classification algorithm (Küppers et al., 2021).
- Fluctuations in the feedrate on a time scale of seconds decrease the grade (Feil et al., 2019).

2.6. Fluctuations

Fluctuations of the feedrate can occur throughout the MRF. Since the facility and sorting units are designed for a certain throughput, fluctuations in the feedrate may influence the sorting performance when the recommended rate is exceeded. Curtis et al. (2021) has proposed to split up the fluctuations into categories based on time: short-term (<15 s), mid-term (15 to 600 s) and long-term (>600 s). The short-term fluctuations can be caused by for example the rotation of a drum sieve or shredder earlier in the process. Mid-term variations may be traced back to discontinuous feeding of the process, while long-term can be traced back to adjustments in the process or previous plant disruptions. Here, the causes of fluctuations identified in earlier research are summed up.

2.6.1. Sorting Process Input

The material that enters the MRF is heterogeneous due to the factors below.

- Quality differences of batches from different municipalities.
- Changes in regulations (deposit scheme, PMD composition, mechanical recovery).
- Retention time at storage locations.
- Bales containing agglomerated material re-entering the process.
- Feeding system of the sorting process.
- Extremely large objects influencing the composition on short term.

2.6.2. System Fluctuations

The design of an MRF and the operating decisions like machine settings may contribute to fluctuations in the throughput throughout the sorting line. In earlier research performed by Curtis et al. (2021) multiple causes of fluctuations were mentioned which are summarised in Table 2.3. The rotational movement in the drum sieve not only leads to fluctuations in the throughput but also the formation of braids. These large and long particle combinations can not be classified correctly by an NIR.

Table 2.3: Overview of fluctuations of the throughput of an MRF and the causes identified in literature.

Location	Fluctuation	Cause	Duration	Frequency	Proposed solution
Human-controlled feeding machinery (wheel loader, shovel etc.)	Batch feeding of shredder	Discontinues feeding with wheel loader.	Mid term	Irregular	Smart control, instructions wheelloader.
Shredder	Bridging	Large particles form bridges in the shredder, making it appear full, influencing the automatic feeding.	Short term to mid term	Irregular	Analysing flow data and machine data.
	Reversing intervals	Shredder settings or obstruction	Short term	30 sec	-
	Reduced processing rate shredder	Large, thick-walled objects are difficult to shred and may block the shredder.	Short term to mid term	Irregular	-
Drum sieve	Fluctuation output	Rotation.	Short term	One drum rotation	Other type of sieve.
	Agglomerated material	Large foils and wires form braids in the drum sieve.		Irregular	Regular maintenance intervals shredder. Iron separation before the drum sieve. Oher type of sieve.

Key Takeaways Chapter 2

- NIR sensor sorting systems are able to distinguish different types of materials and polymers using reflection schemes at high feedrates.
- The working principle, machine design, machine settings and maintenance, influence the range of particle properties which the system can sort correctly when fed in a monolayer. This is referred to as the working range.
- The False Calls can be divided into six types of which some depend on the feed composition, feedrate and/or feeding mechanism.
- The feedrate and feed composition vary through time thus influencing the probability of False Calls.

3

Analysing Sorting Performance

In this chapter, the created framework of False Calls is put to the test in an industrial setting. The goal is to determine the probability of each type of False Call (FC) of a selected NIR sensor system. First, the analysed NIR and the relevant preceding processing steps at the MRF are introduced. Then, the experimental methods are described and finally the results of the analysed NIR are presented.

3.1. Experimental Setup

This research was conducted at an MRF in the Netherlands. At the facility, an NIR was chosen to conduct the experiments. This NIR aims to increase the grade of the mixed plastics product (DKR350) by separating the mixed plastics from the residue. Negative sorting is applied. The targeted materials that are ejected, are all non-plastics and PVC. The non-targeted materials are plastics. This NIR was chosen because the throughput of the NIR is relatively low, which makes manual sampling possible. In addition, mixed plastics are currently the most challenging product at this facility. The mixed plastic product consists of plastic types that are not targeted as one of the mono-products (PS, ABS, etc.) and the losses of mono-products due to the imperfect sorting performance of the preceding steps. The wide range of particle properties of both the mixed plastics and the contamination complicates the separation of unwanted particles from the valuable plastics during this purification step. Mixed plastics is the largest product of this MRF, similar to other Dutch MRF's (Jansen et al., 2015).

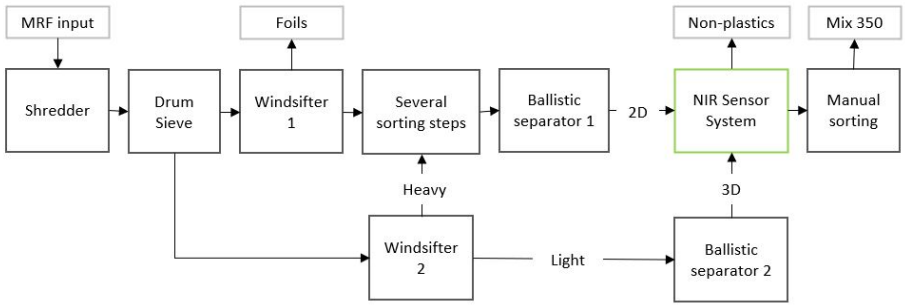

Figure 3.1: Process scheme of sorting steps preceding the analysed NIR (green) and relevant products (gray).

At the start of the sorting process, the material is fed to a bunker using an excavator. Next, in several preprocessing steps the bags are opened and the incoming material is sorted by size and shape (Fig. 3.1). Windsifters separate heavy, mainly thick-walled, 3D particles from light, 2D particles. Since the windsifters are not perfect, heavier materials enter the light material flow and vice versa (Jansen et al., 2015). Ballistic separator 1 consists of two separators in parallel. The NIR analysed in this research is followed up by a manual sorting step. This indicates that the sorting performance of the NIR is insufficient. Due to confidentiality, only the relevant sorting steps and material flows are displayed.

3.1.1. Description NIR Sensor Sorting System

The NIR system is an AUTOSORT TS400, manufactured by TOMRA with a belt width of 2 m. The actuator system contains 80 valves and the belt speed is set at 3.86 m/s. The pressure in the valves is 7.5 bar. The valves are programmed to open 16 ms before the identified particle and close 5 ms after the particle has passed. At the current belt speed this reaction time means that belt area between 0.06 m before and 0.02 m after the particle is targeted by the air nozzle. To prevent the entrainment of non-targeted material into the eject, the spacing between objects should be at least 0.06 m. Material is dropped onto the conveyor belt from two chutes of 0,95 m x 1,20 m and 1,0 m x 1,20m (Fig. 3.2). The material is not equally divided over both chutes; the feed of the chute displayed on the left in Fig. 3.3 also consists of the material flow from Ballistic Separator 2.

Figure 3.2: Feeding mechanism: two chutes drop material on to the belt.

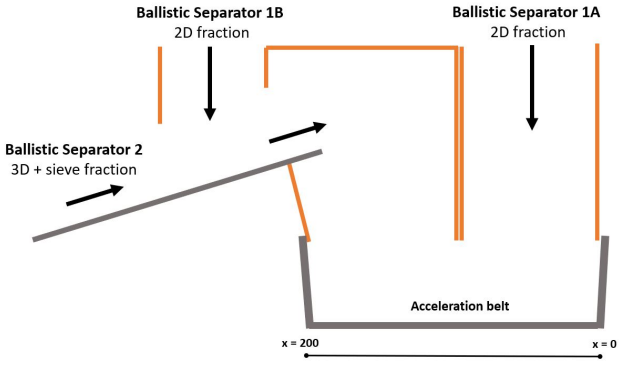

Figure 3.3: Graphic representation of feeding mechanism.

The NIR uses the so-called flying beam technology (Fig. 3.4). The rotating mirror, the defining part of this technology, provides a changing angle of incidence and angle of reflection which enables spectral data collection along the width of the belt. The mirror has a convex polygon shape. The outgoing

and incoming light beams are reflected by a flat side of the convex polygon and the sensor scans from right to left as the mirror turns and both angles increase. At every corner of the mirror the angles of incidence and reflection leap back to the smallest value and the line scan starts over. The incoming light is divided into short time frames and a spectrum is created for the light collected during each time frame. The spectrum is in turn used to assign a material group to the time frame. The rotation angle of the mirror is synchronised to a position along the width of the belt. Therefore, the found material group can be appointed to an area on the belt, which from now on is referred to as a pixel.

This NIR has a spatial resolution of 8 mm, meaning the pixel size is 8 mm by 8 mm. Information is gathered for one line of pixels at a time while the belt and materials pas underneath the sensor. Since the belt width is 2000 mm, one line consists of 250 pixels. The current belt speed requires 482 line scans per second and a time frame of 8.3 nanoseconds per pixel.

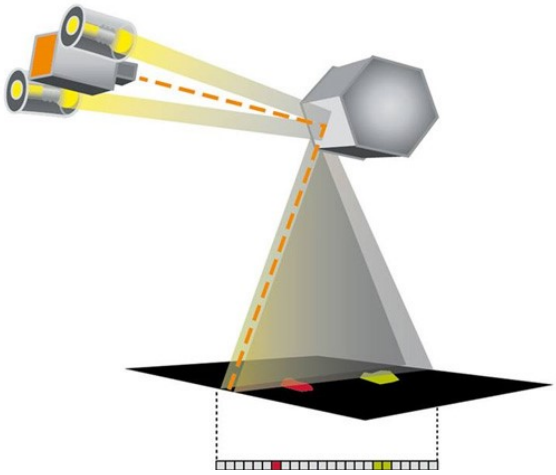

Figure 3.4: Flying beam technology applied in the analysed NIR.

Processing Algorithm

As described in Section 2.4.1, the detected reflection spectrum of a pixel is used to assign a material (class) to that pixel. The classification and processing algorithm are machine specific and vary per producer. The adjustments mentioned in this paragraph are applied in the used NIR.

When the spectrum is not recognised the pixel is left empty at first. Next, using the processing algorithm, the identified materials can be expanded to the surrounding pixels, artificially increasing the positive identified surface. Then, the pixels that remained unidentified are designated as either plastic or non-plastic. This decision is based on the surrounding pixels that are part of a software filter. The following processing algorithm options can be used to adjust the sensitivity per material class:

- Expand the identified material to the surrounding pixels.
- Increase the filter size (standard size is 5 by 5 pixels).
- Adjust the percentage of pixels in a filter needed to assign a material to the filter.

The database contains multiple material groups of both targeted and non-targeted material. When the surface of a particle is not recognised as belonging to one of those material groups and a large share of pixels remains unidentified, the area is classified as 'Others' and is considered a plastic. Non-plastics that are not in the database, therefore, decrease the grade of the product (Fig. 3.5) in this case of negative sorting.

The nozzles are activated when a set number of pixels in an area related to a nozzle is met. The required number of pixels depends on the nozzle distance.

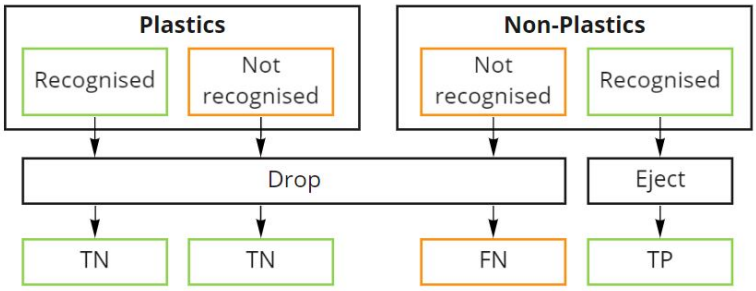

Figure 3.5: Decision scheme of the processing unit.

3.2. Experimental Methods

Five test were designed to single out the probability of each type of FC. This section first provides a description of the analytical methods. Then these methods are applied throughout different tests. Lastly the experiments are set out.

3.2.1. Analytical Methods

The behaviour of the NIR in relation to the feed characteristics was analysed by taking samples, making video recordings and using data collected by the NIR processing unit.

Samples

To analyse the material composition in detail, samples of the material flows were taken on-site. The sorting installation is placed in a large hall where the machines are placed on different height levels. The NIR plastic product falls straight into a chute to the first floor and onto a conveyor belt which ends in the manual sorting cabin. Thus, samples of the product could be taken at the manual sorting conveyor belt (Fig. 3.6a). When sampling, two persons sweep the material of the running conveyor belt into a container while a third person keeps track of the sampling time. The NIR residue is led on in the sorting process. Therefore, the residue could be sampled using a sampling tool that catches the material at a location where the conveyor belt is within manual reach (Fig. 3.6b).

(a) Sampling location of the drop fraction: the manual sorting belt.

(b) Sampling location of the eject fraction: a conveyor belt.

Figure 3.6: Sampling locations

The sampled particles were divided into 13 material classes depending on the type of material, size and shape (Tab. 3.1). The NIR aims to eject all non-plastics and PVC from the material flow in order

for the product to meet the DKR350 standard. Non-plastics and PVC were combined and regarded as one material type. The plastics were split up into rigid plastics and foils because the shape and density are expected to influence the behaviour of the particle in the NIR. The non-plastics show a wide variation of particle properties. Therefore, to decrease the manual sorting work no distinction in shape was made in this category. When uncertainties about the polymer type of rigid plastics arose, staff members of the quality inspection department were consulted to make a distinction between PVC and other types of rigid particles. Before and after the sample analysis, the weight of the total sample was measured. Due to the loss of moisture and small particles, the sample weight may reduce during sampling. When the weight loss remains below 3%, no adjustments or additional samples are necessary (Lebersorger and Schneider, 2011).

Table 3.1: Material classes.

Group number	Material	Size	Shape
1A	Plastic foils	Small	2D/flexible
1B		Medium	
1C		Large	
2A	Rigid plastics	Small	3D
2B		Medium	
2C		Large	
3A	Non-plastics and PVC	Small	All
3B		Medium	
3C		Large	
4B	Plastic particles part of an agglomerate	medium	All
4C		Large	
5B	Non-plastic particles part of an agglomerate	Medium	All
5C		Large	

The diversity of particle shapes complicates the characterisation of particles into size groups. When particles are fed to the NIR only the side facing upwards is visible. Therefore, the particle size and shape of the top view in a stable position are analysed. The following parameters can be used to describe the particle size and shape of irregularly shaped particles (Kandlbauer et al., 2021):

- Equivalent parameters: Dimensions of a chosen geometrical shape of which the area resembles the particle surface area.
- Geometrical shapes: The dimensions of a chosen geometrical shape that encloses the particle.
- Shape factor: Function of the shape perimeter and surface area.
- Feret diameter (minimum and maximum): Distance between two parallel tangents (Fig. 3.7).

It was chosen to divide the particles based on the minimum Feret diameter (F_{min} [mm]) and the maximum Feret diameter (F_{max} [mm]). The F_{min} is important as it is the minimum belt width occupied by the particle if the F_{min} is parallel to the scanline and blow bar. If a targeted particle is too small, the area of the correctly identified pixels may not be large enough to activate the nozzle.

In Fig. 3.8 particles of small and medium-size fraction are shown.

Samples are taken to determine the composition of a material flow, for example, the product of the NIR. The reliability of these samples can be expressed using the sampling error. The required maximum sampling error can be used to determine the sample size. In waste management, a relative sampling error of 20% is accepted. To determine the sampling error for a certain material class the composition of the analysed material flow is approached as a binomial distribution; particles are ei-

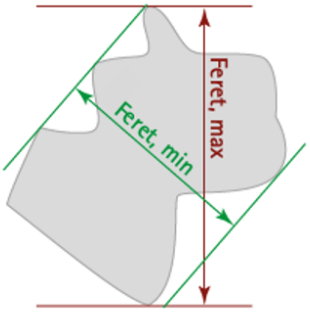

Figure 3.7: Minimum and maximum Feret diameter (Sympatec GmbH, n.d.)

Table 3.2: Assigning particles to particle size groups based on F_{min} and F_{max}

Size Group	**F_{min} [mm]**	**F_{max} [mm]**
Small (S)	<50	<150
Medium (M)	<50	150-300
	50-300	50-300
Large (L)	>0	>300

ther part of this material class or not. This discrete probability distribution is defined by the chance (P) of drawing a particle of the material class. The sampling error is equal to the standard deviation (σ) of the binomial distribution and depends on the total number of particles in the sample (N_{tot}) and the probability (Eq. 3.1a).

However, the value of P is unknown as it is the reason that the sampling analysis is conducted in the first place. Therefore, it is assumed that for a representative sample, the ratio between the number of particles targeted in the sampling analysis (N) and the total number of sampled particles (N_{tot}), resembles P (Eq. 3.1b). When P in Eq. 3.1a is replaced by the ratio of particles, the standard deviation can be calculated using the sampling results (Eq. 3.1d). The sampling error is calculated per material class.

The sampling error σ can be expressed as an absolute error (Eq. 3.1c), a relative error (Eq. 3.1d) or a mass error (Eq. 3.1c). The mass error is calculated using the average particle weight of the found targeted material m_{avg} by dividing the total mass of the targeted material m_t by the number of particles. To determine the required sample size, it is assumed that the share of material targeted during the sampling analysis, P, is always above 0.05. To achieve a σ_{rel} of 20% with P = 0.05, 24 particles should be sampled. This number is rounded to 25 particles. Large particles are likely to account for less than 5% of the particles in the feed. To reduce the manual labour, a higher sampling error is accepted for this size category.

The samples are split into four groups before analysing, if the minimum of 25 target particles is not found in the first share, another quarter is added.

$$\sigma = \sqrt{N_{tot} P(1-P)} \tag{3.1a}$$

$$P = \frac{N}{N_{tot}} \tag{3.1b}$$

Figure 3.8: Examples of the size fractions. Left: Small rigid plastics. Right: Medium non-plastics.

$$\sigma_{\text{samp}} = \sqrt{N(1 - \frac{N}{N_{\text{tot}}})} \tag{3.1c}$$

$$\sigma_{\text{rel}} = \frac{\sigma_{\text{samp}}}{N} \tag{3.1d}$$

$$\sigma_{\text{mass}} = \sigma_{\text{rel}} * m_{\text{avg}} \tag{3.1e}$$

$$m_{\text{avg}} = \frac{m_{\text{t}}}{N} \tag{3.1f}$$

NIR Feed Data

The NIR used in this research collects data about the feed by measuring the (top view) area of all the particles that pass the sensor scan line. The measurements include the distribution of material along the width of the belt [%] of total measured material area] and the material composition based on the area of the material measured from above. A value is given per material [m2/h] and relative to the total belt area occupied by all materials [%].

Video Feed Data

A Nikon 1 S2 is used to record the surface of the conveyor belt. The camera is placed above the belt as shown in Fig. 3.9. Videos with a frame rate of 30 frames per second are made.

3.2.2. Test A: Systemic Errors

To determine the contribution of system errors and the associated chance p_{syst} test runs were performed using clean flakes of PVC and product type plastic. The square product plastic flakes originate from a plastic packaging manufacturer and are made from polyethylene foil (PE) and for the residue PVC flakes were used. The squares have sides of approximately 10 cm. It is expected that the total contribution of systemic errors is around 1%. A total of 100 particles is used for this test in both categories. The particles are fed to the NIR manually to avoid overlap. The test is repeated three times.

3.2.3. Test B: Working Range with Respect to Size Range

An important part of the working range of the NIR is the size range. The machine specification states that the recommended minimal particle size is 20 mm. To confirm, the sorting performance was analysed for square clean particles which in four sizes: 20 mm, 30 mm, 40 mm, 50 mm. In each

Figure 3.9: Camera above the belt

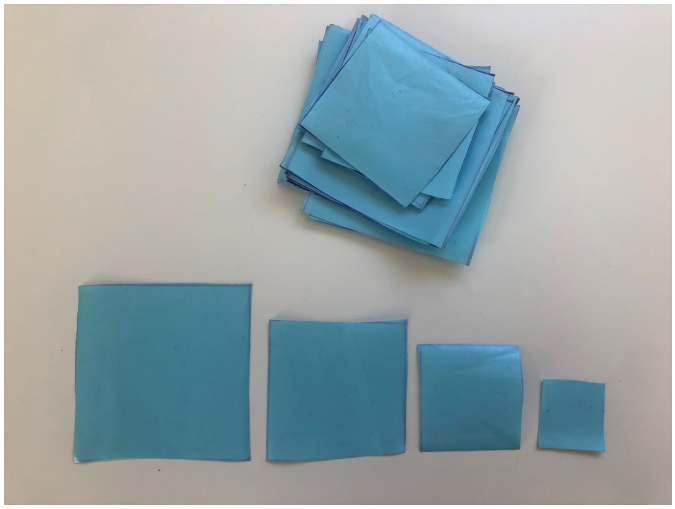

Figure 3.10: Material Test B: PVC flakes

category, 50 flakes are cut from thick-walled PVC. This material was chosen because it is flexible and easy to cut, is well detectable and does not tear like paper. PVC is an eject material. Each run is repeated three times.

3.2.4. Test C: Working Range with Respect to Orientation and Recognition

The goal of this test is to estimate the share of deterministic and stochastic orientation errors. In addition, this test will give an insight into if, and to what extent, deterministic particles, normally always giving an FC, can be processed correctly under normal processing conditions thanks to being overlapped. Finally, an analysis of the deterministic particles provides information on the working range of the sensor and the share of particles with this kind of uniqueness problem.

The deterministic false calls were analysed by NIR sorting four batches of particles multiple times and keeping track of the number of times each particle causes a false call. The material was fed to the conveyor belt manually one by one to exclude overlap errors.

The material that was used for this test was taken from the residue and product flows on the conveyor belts behind the NIR while the MRF was in operation. The four batches represent the four outcomes of the NIR under normal process conditions (Tab. 3.3). By choosing these four batches, the behaviour of deterministic particles under optimal conditions could be compared to behaviour under regular

process conditions. Only the medium and large size fractions were used in these tests to rule out size-related errors associated with the smallest range.

Table 3.3: Material used in Test C.

Batch	Group	Material flow	Material Class
1	FP	Product	Plastics
2	TP	Product	Non-plastics
3	FN	Residue	Plastics
4	TN	Residue	Non-plastics

Deterministic particles always cause a false call under optimal feeding conditions if we look only at orientation and recognition FC's. The non-deterministic particles have a chance between 0 and 1 to be sorted into the wrong fraction which probability is described by Equation 3.2. The total number of runs (k) per batch is 3. The observed numbers of FP or FN per particle (n_{FC}) are recorded.

$$p_{\text{orient},i} = \frac{\text{n}_i}{k} * \text{Share of particles} \tag{3.2}$$

In this test, false calls can be caused by orientation and recognition errors and by systemic errors. This cannot be prevented. To determine the contribution of orientation and recognition errors the results were corrected for the probability that a particle is involved in a systemic error ($p_{\text{syst,n}}$). This binomial chance depends on the found systemic error probability (p_{syst}).

$$p_{\text{syst},n} = \frac{k!}{n!(k-n)!} * p_{\text{syst}}^{n} * (1 - p_{\text{syst}})^{k-n} \tag{3.3}$$

The share of particles in the feed with attributes causing recognition or orientation errors was calculated using the measured sample times. The number of particles per second was determined after which the drop and eject were summed up.

3.2.5. Test D: Feed Characteristics

As discussed in Section 2.5, the feed characteristics influence the sorting performance. The performance of the NIR was tested within the ranges of the feed characteristics found on-site. For example, the performance at the minimum and maximum feedrates were determined. To determine those boundaries the feed was characterised.

Feeding Mechanism and Occupancy Rate

The total area of material on the conveyor belt per unit of time is measured by the NIR. This information was used to calculate the average occupancy rate. In addition, the NIR recorded the distribution of material along the belt. Since the feedrate and the occupancy rate are related, the NIR data of the available occupancy rate is used to inspect the variations of the feedrate through time. An NIR occupancy data set of 20 days is used to ensure that the data is representative and the influence of the varying waste composition is reduced.

Agglomeration

To determine the impact of agglomeration on the sensor performance the occurrences of agglomerated materials in the feed and the composition of agglomerated particles were analysed. A distinction was made between stationary and non-stationary agglomeration. Stationary agglomeration is an umbrella term that is defined as agglomerated particles that do not separate when shaken by hand. This

term includes multiple mechanisms such as metal cans locked around other material and unopened bags. This type of agglomeration is assumed to be present in the input of the MRF. Non-stationary agglomeration, on the other hand, is material that is hooked into each other due to shape or sticky surfaces. This kind of agglomeration is likely to be formed inside the sorting process and can be separated by some shaking.

The stationary agglomeration analysis is combined with the analysis of the samples of Test E. Stationary agglomeration is characterised by the following variables:

- Number of agglomerated particle combinations (at least 2 particles).
- Weight of the agglomerates.
- Composition of the agglomerates (targeted/non targeted material) in both the number of particles and weight.
- Agglomeration mechanisms.

The non-stationary agglomeration was analysed by taking 8 visible heaps from the product. The reason is that earlier performed on-site observations indicated that non-stationary agglomeration is likely to enter the plastic product. The frequency of non-stationary agglomerates was determined by analysing video recordings.

Non-stationary agglomeration is characterised by the following variables:

- Weight of agglomerated particles.
- Mass composition of agglomerated particles (targeted/non targeted material).
- Agglomeration mechanisms.
- Occurrence rate.

3.2.6. Test E: Occupancy and Overlap

Design of Experiments

The FC caused by overlapping materials were determined using the Design of Experiments (DoE) method. This method is essentially a regression analysis that provides a guideline on how to plan and design a test. It is therefore an efficient way to observe the effects of multiple parameters simultaneously, together with the interactions of the factors. Performing experiments in an industrial setting can be costly. Alterations to the operation settings of the MRF such as an adjustment of the MRF feedrate influence the quantity and quality of the product. In addition, analysing samples is time-consuming which makes efficiency is essential. DoE has been applied before in the evaluation of the performance of a shredder for a heterogeneous waste input and was found to provide significant models (Khodier et al., 2021). The parameters that affect the system and can be set during the experiment are called factors in DoE terminology. The parameters that describe the output of the system are referred to as responses.

Full Factorial Design

A commonly applied experimental design is the full factorial design. In this design the responses are measured for all combinations of input factors at both high (1) and low (-1) levels. Consequently, a full factorial design with k factors requires at least 2^k runs. The design can be strengthened with the response of the system with both factors set to level 0. These so-called center points can be added to check if the relationship between the factor and the response is truly linear or if a curvature exists. Furthermore, the influence of uncontrollable parameters during the experiment can be estimated using center points.

It is assumed that interactions between the two factors (X_1 and X_2) may influence the responses (Y_r). Therefore a polynomial multilinear model is chosen to determine a best fit to the data as follows:

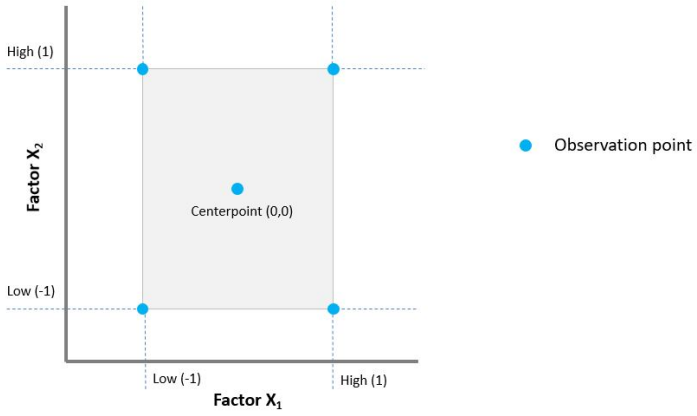

Figure 3.11: Full factorial design, k=2

$$Y_r = \beta_0 + \beta_1 X_1 + \beta_2 X_2 + \beta_3 X_1 X_2 + \epsilon \tag{3.4}$$

The equation consists of a constant, β_0, two main effects and one two-factor interaction. The coefficients are indicated with β.

Experimental Design
It was hypothesized that the feedrate, the feeding mechanism and the percentage of foils affect the amount of overlap. The goal of this experiment is to investigate the possible relationship between these factors and the errors caused by overlapping materials. Doing so, the feeding mechanism was kept constant and the feedrate and feed composition were chosen as factors (k = 2). Three centre points were added to the design which ads up to total of seven runs.

The feedrate of the NIR is varied by adjusting the input of the MRF to a value between 50% (-1) and 100% (1) of the original feedrate of the MRF. The material composition and amount of targeted material are controlled using the settings of Windsifter 1 (Fig. 3.1).

This windsifter removes materials with a low density - mainly foils - from the flow towards the NIR. By adjusting the settings, the share of foils continuing to the NIR can be controlled.

The principle is demonstrated in Fig. 3.12. The airflow from below can be controlled using valves. The heavy fraction continues to the NIR. If the blow valves are closed, fewer foils will be blown into the light fraction, increasing the share of foils in the heavy fraction and reducing the share of non-plastics towards the NIR. In the DoE format, an open valve corresponds to level -1 and a closed valve to level 1.

Table 3.4 shows the operational setting for each run and the run order.

The test was conducted during the same 8-hour shift to avoid changes in operating staff to reduce outside parameters that may influence the experiment. For example, a different wheel loader may load the MRF in another way influencing the MRF feed. Also, two members of the operation staff assist during sampling. At the beginning of each run, the MRF throughput and the windsifter settings were altered. To make sure the flow throughout the facility was stabilized for the new settings, the samples were taken 40 minutes after the changes.

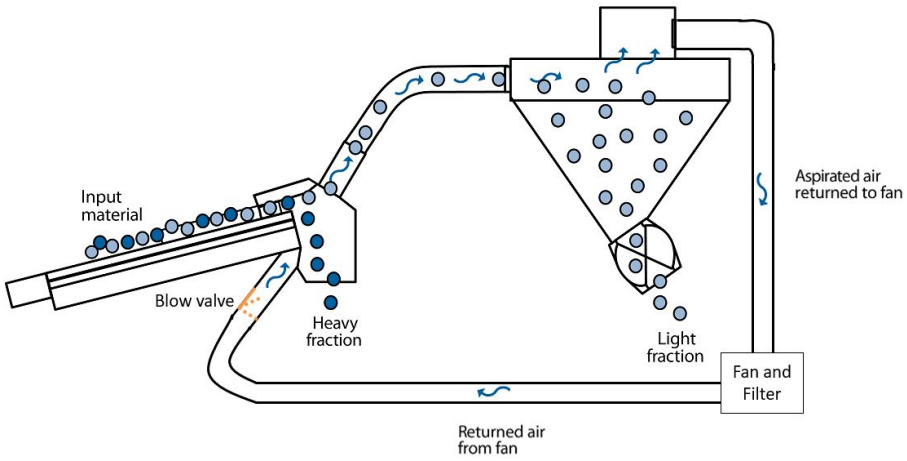

Figure 3.12: Simplified image of windsifter comparable to windsifter used on-site. The blow valves control the amount of returned air from the fan ((Nihot Airconomy, n.d.)).

Table 3.4: Overview of DoE runs and operational settings

Run	Throughput		Windsifter blow valves	
	Level	Factor setting [%]	Level	Factor setting
1	0	75	0	half opened
2	-1	50	-1	open
3	-1	50	1	closed
4	0	75	0	half opened
5	1	100	-1	open
6	1	100	1	closed
7	0	75	0	half opened

The following three principles of DoE were implemented in this experiment:

- Replication: multiple measurements of the responses for the same combination of factors should be made over a period of time. This is different from multiple measurements at the same moment, which are just repeated measurements. The replication aims to capture the amount of random noise caused, for example by variations in the feed that are not measured. In this research three replications of the so-called centre point were performed: at the beginning, the middle and the end of the experimental runs.

- Blocking: If part of the system changes throughout the experiment, such as a different operator, the experiment should be split into separate blocks, blocking in DoE terminology. This means that the experimental runs are repeated for both operators.

- Randomization: to reduce the bias of the sampler, ambient light or the influence of variations in the performance of sorting units earlier in line than the NIR, the order in which the experiments are performed, should be random except for the centre points.

Data Collection
During each run, three samples are taken of both the product and the residue. The sampling time was recorded. The following values were measured for the three size classes in both mass and number of particles:

- Share of foils
- Share of rigid material
- Share of contamination
- Stationary agglomeration including the share of contamination in the agglomeration. Agglomeration is only measured for medium-sized and large particles.

These values are used to calculate the following eight responses (Y_r):

1. Average feedrate of NIR (Eq. 3.5a and Eq. 3.5b).
2. Share of non-plastics in the NIR feed.
3. Share and grade of agglomeration in the NIR feed.
4. TPr (Eq. 2.1a)
5. FPr (Eq. 2.1b)
6. Grade (Eq. 2.2a)
7. Recovery (Eq. 2.2b)
8. Mass recovery (Eq. 2.2c)
9. Discharge (Eq. 2.2d)

The feedrate and feed composition were calculated by combining the values found for the product and residue. To determine the average mass feedrate $\dot{m}_{\text{feed}}$ [kg/s] the mass flow to both outputs was calculated.

$$\dot{m} = \frac{\sum_{n=1}^{3} \frac{\text{Sample mass}}{\text{Sample time}}}{\text{number of samples}} \tag{3.5a}$$

$$\dot{m}_{\text{feed}} = \dot{m}_{\text{drop}} + \dot{m}_{\text{eject}} \tag{3.5b}$$

Analysis of Results

The feedrate of the MRF was altered to indirectly influence the feedrate of the NIR because the latter could not be adjusted individually. Experimental data analysis occurred in two steps. First, the influence of the factors, the MRF feedrate and the opening of the blow valves, on the feedrate of the NIR and the share of non-plastics in the NIR feed were analysed. Due to the processing steps between the start of the MRF line and the NIR it is likely that the factors are not one on one related to the feed characteristics of the NIR. Next, the effect of the feedrate and the share of targeted material on the TPr, the FPr and the grade were analysed.

The factors were substituted into Equation 3.4, which was used for the regression analysis. Before the experiments, it is unknown if a statistically relevant relation can be found between the MFR feed (F) and the settings of the windsifter (W) and the responses (Y_r).

$$Y_r = \beta_0 + \beta_1 F + \beta_2 W + \beta_3 FW + \epsilon \tag{3.6}$$

The statistical software MiniTab® was used to evaluate the data. The software conducts a regression analysis and visualises the results. For each response, forward selection is applied to create a statistically significant regression model. The software calculates the p-value of each term which indicates the empirical significance. If the p-value is below a chosen significance level (α), it implies that the response is not likely to be random. The value of the response can then be predicted using the coefficient and the input factor. When forward selection is applied, first the term with the lowest p-value is added to the model, followed by the others until only terms higher than the chosen significance level remain. In general, a value between 0.05 and 0.15 is assigned to α. In this research a value 0.1 is chosen, similar to the value applied by Khodier et al. (2021) during their experiments with waste.

Once a model with significant terms for a response is created, an analysis of the variance (ANOVA) is performed. The share of variation of the response that can be predicted using the input factors is described using the coefficient of determination (R^2). R^2_{adj} is the coefficient of determination adjusted for the number of variables in the model.

Material Classification Overlap
To create a better understanding of the classification of overlapping material, multiple particle combinations were placed underneath the light beam of the NIR on the switched off conveyor belt. The reaction of the actuator was confirmed by listening if the valves eject air. The results can not be used to conclude whether or not both particles are truly ejected when targeted by the nozzles. The following combinations were tested:

- Non-plastic material - Plastic foil (single layer).
- Non-plastic material - Plastic foil (multi-layer).
- Non-plastic material - Rigid plastic (overlapping).
- Non-plastic material - Rigid plastic (nearby).

3.3. Results

3.3.1. Test A: Systemic Errors

The systemic error is found to be around 2% for plastics and 4% for non-plastics. It is observed that the PVC particles are classified incorrectly due to at least three phenomena:

- The airflow of a nozzle is temporarily insufficient.
- The nozzles do not react to the PVC particle at all due to either failure of the sensor, the software or the nozzles.

Table 3.5: FPr of clean PP flakes and FNr of clean PVC flakes.

Particle Material	Amount of Particles [nr]	False Call Rate [%]			
		Run 1	Run 2	Run 3	Average
PP (Product)	100	2	0	4	2
PVC (Residue)	100	4	5	4	4

3.3.2. Test B: Working Range with Relation to Size

In Fig. 3.13 the TPr for square particles with a size up to 50 mm is shown. It is clear that particles with a side length of 20 mm, the minimum particle size according to the specifications, are not classified correctly. The nozzles did not react to this particle size, hence it is assumed that this size is not correctly identified by the classification algorithm. Next, as the size increases, the TPr increases from an average rate of 44% for 30 mm to 65% for 50 mm. This means that working range size errors are deterministic if they are below a certain size. For larger sizes the performance improves but is not as expected. It is proposed to determine a cut-off value equal to the minimal size based on the TPr.

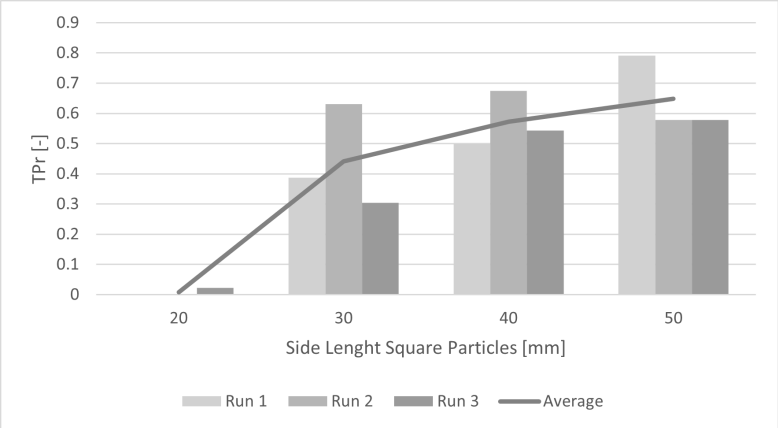

Figure 3.13: Sorting performance for square eject particles with a size up to 50 mm.

3.3.3. Test C: Working Range with Relation to Recognition and Orientation

Four batches of particles were sorted multiple times to identify the deterministic and stochastic errors related to orientation and recognition errors. In Table 3.6, the results of the batch of False Negative material are presented. These particles were meant to be ejected, however, it can be concluded that 49% of the particles in this batch are not ejected in any of the three runs. Out of those 28 particles, 8 were not correctly identified when placed under the sensor on the non-moving conveyor belt. In Fig. 3.14, a few of these particles are displayed. The results also show that 17% does not cause a FN in three out of three runs. Under processing conditions, these particles might have been overlapped and

dropped together in the plastic product, causing a FN. Another smaller chance is that these particles had a low chance of an unfavourable orientation.

In Appendix A the results of the other batches are displayed. All plastic particles (TN and FP) were classified correctly by the sensor when placed on a non-moving belt. As can be seen in Table 3.8, a total of 6% of the medium and large plastic particles were involved orientation errors.

Table 3.6: Number of False Positives per individual particle after 3 batch runs. Batch Material: False Negatives

Number of FN/runs	Number of particles [nr]	Share of total particles [%]
0/3	10	18
1/3	7	12
2/3	12	21
3/3	20	35
3/3 (Classification error)	8	14
Total	57	100

In Table 3.7 and Table 3.8, the results of the batches are combined and processed. The chance of an orientation error or recognition error is much higher for non-plastics. This could be due to the processing algorithm; materials that are not recognised are classified as plastics and dropped. Also, the material characteristics vary more for non-plastics than plastics, making it harder to include all such material types in the database. Orientation errors due to movement on the belt can also only be determined for non-plastic materials. If a plastic particle has a relative speed, it will still be dropped if it does not arrive at the expected time because the belt is empty and the nozzles are not activated at all.

Table 3.7: Orientation and sensor errors of non-plastic particles.

Number of FN/runs	Share of particles [nr.%]	Systemic errors	Correction	p_{orient}
0/3	25	88.5%	37%	0.00
1/3	14	11.1%	3%	0.01
2/3	21	0.5%	20%	0.13
3/3	31	0.0%	31%	0.31
3/3 (Classification error)	11	-	11%	0.11

Table 3.8: Orientation and sensor errors for plastic particles.

Number of FN/runs	Share of particles [nr.%]	Systemic Errors	Correction	p_{orient}
0/3	89	94.1%	95%	0.00
1/3	6	5.8%	0%	0.00
2/3	3	0.1%	3%	0.02
3/3	3	0.0%	3%	0.03
3/3 (Classification error)	0	-	0%	0.00

During the test, the particle characteristics were noted and recordings were made of the orbit of the particles after ejection. Below the observed causes of orientation and sensor errors are listed.

Observed errors due to non-plastics orientation and recognition:

- Packaging consisting of paper and plastic.
- Contaminated tetra pack.
- Medical plastic items.

- Light paper sheets.
- Heavy particles (e.g. diapers).
- Cables and other long and thin wires.
- Packaging with content (Uniqueness error).
- Black materials.

Plastics orientation errors:

- Round plastic lids.
- Contaminated foils.
- Plastic packaging with large paper labels.

Figure 3.14: Deterministic particles found in the plastic product.

3.3.4. Test D: Feed Characteristics

Feeding Mechanism and Occupancy Rate

The data collected by the NIR gave a first impression of the variations in feedrate. Temporary stops of the MRF processing line were removed from the data set. The sensor system measures the material area that passes underneath the sensor for a total time of 5 minutes. So, short and mid-term fluctuations can not be distinguished when using these data. The data were applied to check if the feedrate during Test E matches the ranges found during normal process conditions. Fig. 3.15a shows an average of just below 5000 m^2 per hour and no outliers at the top. Using the belt width and the belt velocity the average occupancy density is calculated to be 18%.

The 5-minute average area of non-plastic material varies between 12 % and 27% of the total material feed area.

The NIR is fed by two chutes which widths lead to the two peaks loadings along the width of the belt (Fig. 3.16). On the right (position 150 cm), the occupancy rate is highest. That side corresponds to the chute in which 2 feed material flows are combined (See Fig 3.3). The graph shows the distribution of the measured area of the feed along the belt width. The average occupancy density is 18% and the occupancy density at the peaks is even higher. It is concluded that the occupancy rate along most of the belt width exceeds the 7.5% free rectangular particles can occupy without overlap Wen et al. (2021). Since the feeding mechanism is not altered, this uneven belt distribution is a continuous problem.

Stationary Agglomeration

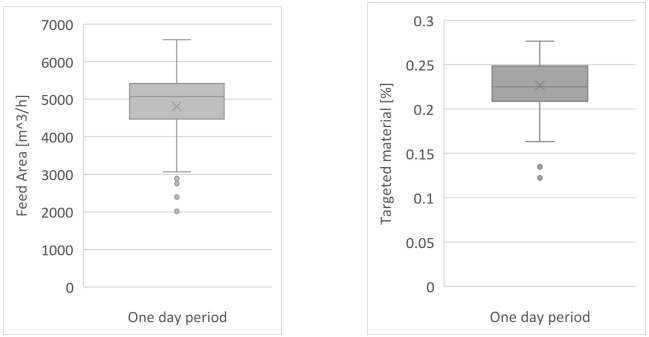

(a) Five minute average of the feed surface area during one day

(b) Share of non-plastics material of the feed surface area during one day

Figure 3.15: Range of feed characteristics.

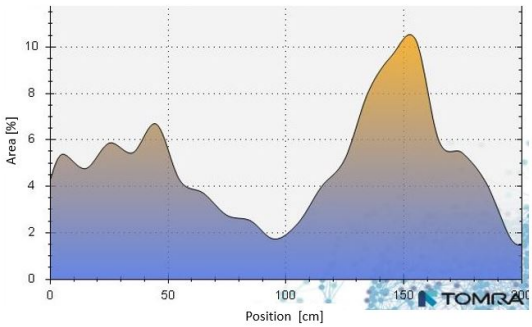

Figure 3.16: Distribution the total measured material area along the belt width of the NIR during a one day period.

Some particles are part of a group that should not be presented to the sensor in a monolayer. The occurrence of different agglomeration mechanisms was determined in relation to the total amount of stationary agglomeration. A total of 35 agglomerated groups were detected and analysed. Based on the results it is concluded that locking is the most occurring type of agglomeration mechanism (Fig. 3.17). Still, this mechanism accounts for only 23% of the non-plastic particles found in agglomeration and 12% of the mass. Unopened bags are the largest contributor of agglomerated non-plastic particles and total agglomerated mass.

It was found that on average 13% of the NIR feed mass consists of stationary agglomerated material (Tab. 3.9) with an average non-plastic content of around a third of the mass and a fifth of the particles. However, large variations occur for both shares.

Table 3.9: Stationary agglomeration in the feed.

	wt.%	**nr.%**
Average agglomeration in feed	13	5
STD Aggl/feed	6	2
Average Non-plastics in agglomeration	31	22
STD non-plastics	11	6

Non-Stationary Agglomeration

In Table 3.10, the composition and mechanisms of 8 agglomerate groups are listed. On average 69% of the non-stationary agglomerate mass consists of plastics, which is quite similar to the feed composition. Video recordings show that non-stationary agglomeration can start with one single particle

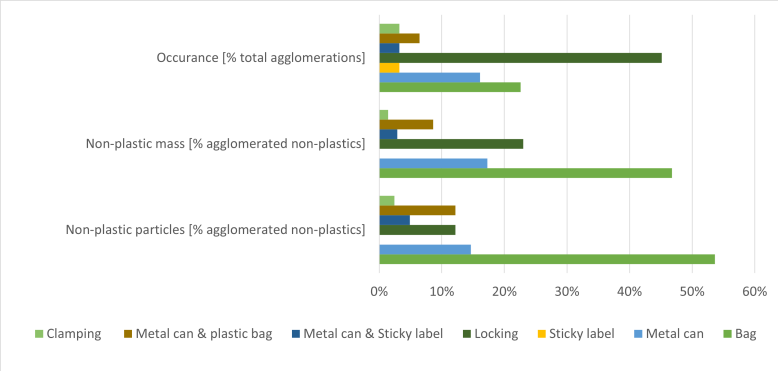

Figure 3.17: Stationary agglomeration mechanisms.

that is stuck on the side of a chute and then can grow to an agglomerate covering an area of 1 m^2 in 8 minutes.

Table 3.10: Non-stationary agglomeration in the product.

Total weight [kg]	Weight FN [kg]	Grade [wt.%]	Agglomeration mechanism or material
2.36	0.46	81	Rope, hook of hanging planter, bag in bag, adhesive material, pantyhose, torn up planter, iron hooks
0.39	0.12	69	Copper cable, rope, torn up material with rough edges
0.30	0.09	70	Iron/plastic wire
1.89	0.92	51	Rope, textiles
0.61	0.24	61	Material with sharp edges
0.59	0.25	58	Wire
0.14	0.04	71	Iron wire, garbage bag loop
0.53	0.00	100	Bags inside bag
6.81	2.12	69	

3.3.5. Test E: Overlap and Feedrate

The regression analysis of the experimental data of Test E indicated that, as expected, a statistically significant relationship exists between the NIR feed and the input factors for both particle and mass measurements (Tab. 3.11). An interaction was found between the input factors meaning that at higher MRF feedrates and closing of the blow valve in the windsifter, the effects on the NIR feed are amplified (Fig. 3.18). Also, the regression analysis implies that when the throughput is high, the amount of non-plastics in the NIR feed decreases when the valves are closed, as aimed for (Fig. 3.19). However, at low MRF throughput rates, closing the valve leads to an increase of non-plastic particles. Therefore, it is concluded that adjusting the position of the blow valves is not a suitable way to vary the number of non-plastics.

Table 3.11: Results of the regression analysis: model coefficients and ANOVA values.

Coefficients	Feed [nr/s]	Feed [kg/s]	Non-plastic [wt.%]	Non-plastic [nr.%]	Foils [wt.%]	Foil [nr.%]	Rigid [nr.%]
Constant (β_0)	58.5	-0.23	0.359	0.033	0.695	1.015	-0.017
Feed (β_1)	1.4	0.02	-	0.003	-0.003	-0.006	0.002
Wind (β_2)	-0.4	0.01	-0.001	0.003	-	-0.004	-
Feed*Wind (β_3)	0.02	-	-	-3.5E-05	-	3.9E-05	-
			ANOVA				
R^2	96.0	82.9	46.1	93.4	94.6	95.2	84.9
R_{adj}	91.9	74.4	35.4	86.7	93.5	90.4	81.9
p_{Mod}	0.01	0.03	0.09	0.03	< 0.001	0.02	0.003

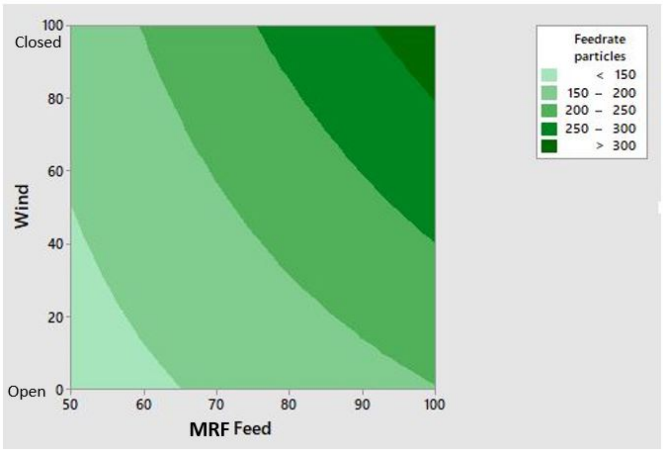

Figure 3.18: Effect of the input factors on the feedrate [nr/s].

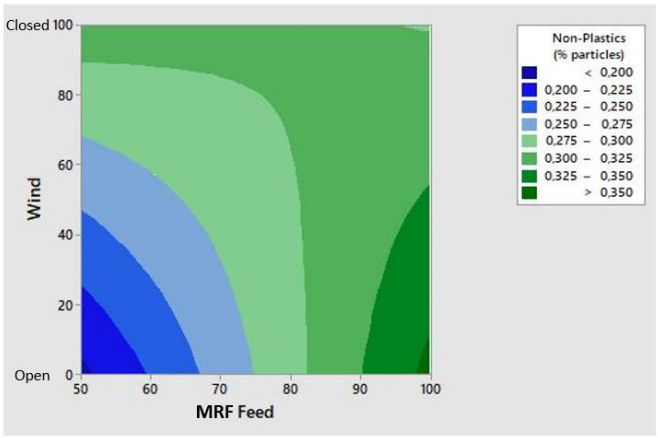

Figure 3.19: Effect of the input factors on the share of non plastic particles [nr.%].

Finally, the fraction of rigid particles and foils in the NIR feed is influenced by the feedrate. It is likely that a lower throughput rate improves the ballistic separation performance and decreases the amount of rigid plastics in the NIR feed. The material composition and size fractions of the NIR feed in all seven runs can be found in Appendix A.

For the mass fraction of rigid plastic particles, the p_{mod} was higher than 0.1 thus no significant relation was found. Also, the coefficient of determination for the mass of non-plastic particles is very low and the model prediction is considered insignificant.

The feed composition was used to calculate multiple performance indicators such as the grade and the TPr of the material classes (Tab B.1, Appendix B). The performed regression analysis results in significant models for the TPr of particles and mass (Tab. 3.12). The R^2 and R_{adj} are higher for the medium size fraction than for all non-plastic particles combined. This indicates that the model prediction of the TPr of the middle size fraction using the input factors is better than the prediction for the TPr of all particles.

An increase in feedrate lowers the mass TPr. When the blow valves are closed, the decrease is steeper (Fig. 3.20a). This is not the case for medium-sized non-plastic particles (Fig. 3.20b) as will be discussed in Section 3.3.6.

Material Classification in Case of Overlaps

Table 3.12: ANOVA

	TPr [nr.%]	Discharge [wt.%]	TPr medium sized NP [nr.%]
Constant (β_1)	0.3476	0.4227	0.373
Feed (β_2)	-	-4.6E-05	0.00056
Wind (β_3)	-0.00142	0.000381	0.00156
Feed*Wind (β_4)	-	-2.1E-05	-0.000035
		ANOVA	
R^2	70.79	96.95	84.61
R_{adj}	64.95	93.89	69.22
p_{Mod}	0.018	0.009	0.098

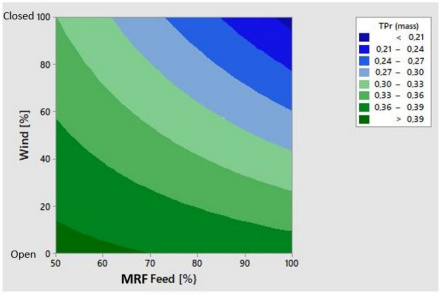

(a) Effect plot: TPr Non-plastic medium size fraction [nr.%]

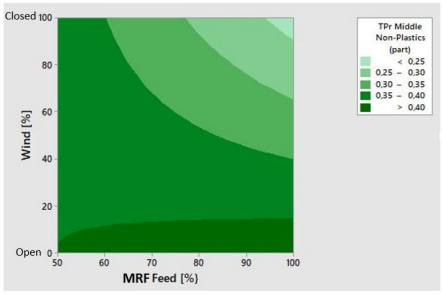

(b) Effect plot: TPr Non-plastic medium size fraction [nr.%]

Multiple combinations of particles were placed on the non-moving belt of the NIR feed (Fig. 3.21). It was found that the actuators were activated when non-plastic material is placed underneath a single layer of plastic transparent foil but not when the non-plastic is underneath multiple layers of transparent plastic foil. Also, a slight overlap of the non-plastic material by rigid material may already prevent actuator action.

3.3.6. Discussion

In this chapter a framework of the causes of false calls of an NIR was introduced and applied to an NIR in an MRF. All errors observed and identified while testing could be assigned to one of the FC categories. In this section each category will be discussed to determine the accuracy and evaluate the results.

Systemic errors

The systemic error of the NIR is higher than the 1% that was expected beforehand based on earlier results of preliminary test performed by Küppers et al. (2020) using clean flakes. It was observed that insufficient airflow inhibited correct classification of the PVC particles. This is likely due to fouling and could be prevented by adequate maintenance. Research has shown that failing of 20% of the air valves reduces the TPr with 20% (Küppers et al., 2021). The larger the share for failing air valves, the higher the probability of systemic errors.

Size errors

PVC particles below a size of 20 mm are not classified correctly by the NIR as indicated by the manufacturer. As predicted, the the TPr increased along with the particle size increased. In this research square particles up to 50 mm were analysed. But at a size of 50 mm the average TPr is still only 65% . Due to a lack of time particle sizes between 50 mm and 150 mm were not analysed. In addition, only square particles were used as feed hence TPr of thin particles remains unknown.

The TPr varies per run per size with differences as big as 30% for a size of 30 mm. The same batch of

(a) Single-layer foil: shoot.

(b) Multi-layer foil: no shoot.

(c) Rigid small overlap: no shoot.

(d) Rigid no overlap: shoot.

Figure 3.21: Classification and actuator action by overlapping of materials.

PVC flakes was used for all three runs. The flakes were wiped clean in between the runs but dirt may have adhered to the surface.

Recognition and Orientation Errors

Recognition and orientation errors were determined in the same test. In this industrial setting, the classification data per pixel is not available to the users of the NIR. Therefore, in some cases, it was not possible to determine if a particle was not recognised on the moving conveyor belt or if it has a high probability of an orientation error. When these particles were placed on a non-moving conveyor belt, the nozzles were not constantly opened but sputtered. These particles were assigned to orientation errors.

Overlap Errors

The regression analyses of the experimental results of Test E showed that in general, the TPr decreases with an increase in feedrate which corresponds to the trends found in literature. However, this was not the case for the particles in the medium size fraction with closed blow valves of the blow valves. This can be explained by looking at the effect of both input factors - the MRF feed and the position of the windsifter blow valves - on the share of non-plastics in the feed (Fig. 3.19). When both input factors are set to level 1, the share of non-plastics is at its highest point. In earlier research, a relation was found between the share of non-plastics and the TPr in the mining industry but not in the waste sorting. However, the decision to eject a particle is also influenced by the processing algorithm. The

NIR is programmed to give priority to rejecting material. A larger share of plastics leads to an increased chance of a non-plastic particle being overlapped by a plastic particle likely resulting in a drop of both particles. But since the share of non-plastics was not systemically influenced, more research is needed to identify the influence of the processing algorithm on the relationship between the share of non-plastics and the TPr.

Even though a significant relation was found between the feedrate and the TPr, the feedrate did not influence the grade or recovery, in contrast to earlier performed research. Based on the performed tests, it is concluded that correlations between the NIR feedrate and feed composition and the sensor performance found in earlier research do not necessarily apply to waste sorting in an industrial setting. In a lab setting where thick rigid particles are used, the eject or drop decision depends on the particle on top. But when transparent foils are involved, the sensor might also identify the particle underneath. Also, the processing algorithm can influence the outcome.

Another explaination for the absence of the expected relations between the feedrate and the recovery could be the design of the experiment. It was aimed to keep all variables except for the input factors stable. However, changing the throughput rate of the MRF can have a significant effect on the performance of all preceding sorting steps. For example, it was found that the share of rigid plastic particles in the feed is related to the feedrate of the MRF. A lower feedrate may lead to better performance of the ballistic separator and therefore a smaller fraction of rigid plastic particles. Further, it was found that the non-plastic medium-sized particles in the sensor feed have a lower average particle weight (Appendix B). This too could indicate better sorting performance of the ballistic separator at lower feedrates. A higher average particle weight can lead to a different trajectory once ejected and therefore affect the sensor performance. However, more research is needed to demonstrate the effect of the feedrate of the ballistic separator on the average particle weight. Nevertheless, unforeseen effects of the preceding processing steps altered the feed composition and may have influenced the sorting results. Khodier et al. (2021) stated that the DoE method can be applied to experiments using heterogeneous waste. However, unlike in the experimental design of Khodier et al., multiple preceding sorting steps could influence the feed composition. It is therefore recommended to create an artificial feed using real waste samples. However, at this facility, it was not possible to feed a prepared batch to the NIR through both chutes without other sorting steps in between. Therefore, the model of the NIR created in this research uses the MRF feed as an input factor instead of the NIR feed.

In addition, the sampling method may have led to deviations in the results compared to the real feed composition. First of all, because the samples of the drop and eject fraction were taken in a short period but not simultaneously.

Key Takeaways Chapter 3

- Five tests are performed on-site to single out the probability of each type of False Call per material class.
- The Design of Experiments method is applied to analyse the effect of the feedrate and feed composition on the overlap errors.
- As expected, the probability of being involved in a False Call due to size decreases when particle size increases for particles <50 mm.
- The probability of being involved in an orientation or recognition error is determined to be around 50% for non-plastic particles and 3% for plastic particles.
- The TPr of non-plastics does not exceed 45%, meaning that more than half of the contamination present in the feed ends up in the product.

4

Statistical Model

In this chapter. a MATLAB implementation of the statistical behaviour of the NIR sensor system is introduced. This implementation is based on the FC parameters in Fig. 2.4. The experimental results from this research concerning the possible FC's were applied. This model allows us to simulate different optimisation scenarios. Then, multiple feed optimisation scenarios were tested. Overall, this model is aimed at improving the understanding of how all the different types of errors come together and affect the sorting performance. Three scenarios are designed to investigate if, and to what extent an adjustment to the present NIR could improve the performance.

4.1. Scenarios

Once the overlap probabilities are determined, three scenarios are implemented. These options are chosen because they are realistically possible to the present MRF and tackle at least one type of error. In the first two scenarios the feed characteristics are altered. The third scenario involves an adjustment of the sensor system. An overview of MRF process improvement suggestions will be presented in Chapter 5.

1. Narrow Size Distribution: In the previous chapter the working range was analysed. It was found that the NIR has a lower TPr for small particles. In this first scenario, the input feed was modified to simulate the effect of removing a large part of the small particle size fraction. In the MRF, a more narrow size distribution may be achieved by sieving the feed. The parameters that describe the particle size distribution in the model are adjusted.

2. Tackling Stationary Agglomeration: Stationary agglomeration largely consists of unopened bags (Section 3.3.4). More bags may be opened correctly by adjusting the bag opener settings or placing an additional bag opener before the sensor sorting system. In this scenario it was assumed that a modification in the preceding MRF line leads to more correctly opened bags. This can reduce the share of stationary agglomeration in the input by 50%.

3. Reducing Classification and Orientation Errors: When particles outside of the working range are fed to the sensor system, classification and orientation errors are likely to occur. In this last scenario, instead of adjusting the feed, the working range of the sensor system was expanded. The working range may be improved by placing a Laser Object Detection (LOD). This type of sensor can detect if an object is present on the belt by height differences. This enables the detection of black particles and materials that are not available in the database. The NIR sensor software is also able to detect the

presence of particles that are not part of a certain material group or the conveyor belt and classifies this as 'Others'. But the current software can not eject materials identified as 'Others' (Fig. 3.5). Hence the processing algorithm should be adjusted to enable the ejection of unknown materials.

However, the application of a LOD or an adjustment of the processing algorithm do not eliminate all classification and orientation errors. For example, the blow bar is still not able to move heavy particles over the splitter. Therefore, it was assumed that the classification errors reduce by 90% and the orientation errors by 50%.

4.2. Conceptual Model

The model is created in MATLAB and revolves around a system matrix of n by m, where n is the number of particles. In the first column, the type of material is assigned to each particle in the simulated heap which consists of 10000 particles. The particle groups introduced in Table 3.1 in Chapter 3 are used: foils, rigid plastics, non-plastics, and plastics and non-plastic that are part of an agglomerate. In the next two rows, two Feret diameters F_1 and F_2 are given to each particle using a group-specific Weibull distribution. The lowest of the two values represents F_{min}, the highest F_{max}. Then, columns 4 to 10 represent the probability of the different types of false calls. Depending on the information in the first three columns, each particle has the probability of either causing an error (1) or not causing an error (0), in each column representing a type of FC. In the second last column the values of columns 4 to 10 are summed up to give the total number of FC's the particle is involved in. A value of 1 or higher means that the particle in the corresponding row is sorted incorrectly due to FP or FN. Finally, the last column contains the information about the particle weight which is in turn used to determine the grade, recovery and mass recovery.

A Monte Carlo analysis was performed, meaning that the model was run multiple times with random input composition taken from the earlier determined normal distribution (Tab. 4.2). The mean values and standard deviation of the output values were determined. The total number of runs was set to 1000. This number was determined by increasing the number of runs in steps of 10 and comparing the mean values of the results. At 1000 runs the swaying of the mean values is reduced to a minimum (Fig. Appendix C)

$$\begin{bmatrix} x_1 & F_{1,x_1} & F_{2,x_1} & p_{syst,x_1} & p_{size,x_1} & p_{class,x_1} & p_{orient,x_1} & p_{over,x_1} & p_{over,st,x_1} & p_{over,nst,x_1} & p_{tot,x_1} & m_{x_1} \\ \vdots & \vdots & \vdots & \vdots & \vdots & \vdots & \vdots & \vdots & \vdots & \vdots & \vdots & \vdots \\ x_n & F_{2,x_n} & F_{2,x_n} & p_{syst,x_n} & p_{size,x_n} & p_{class,x_n} & p_{orient,x_n} & p_{over,x_n} & p_{over,st,x_1} & p_{over,nst,x_1} & p_{tot,x_n} & m_{x_n} \end{bmatrix}$$

4.2.1. Assumptions

- Small particles are not involved in orientation errors or sensor errors, these are accounted for by the size errors.
- Particles do not result in an orientation error and a recognition error simultaneously.
- In Test E results such as the average feedrate, grade and recovery were determined without the effect of non-stationary agglomerate. To simulate the impact of the non-stationary particle combinations on the sorting results, they are added on top of the average feed. Therefore, the total amount of sorted particles in one run exceeds 10000. In the model, the addition does not affect the probability of overlap errors.
- Particle size is only important for free particles since they cause errors based on size.

4.2.2. Input Parameters

The probabilities of each type of false call determined in this research were implemented in the statistical model (Tab. 4.1).

Table 4.1: False call probabilities with monolayer feeding derived from experiments

Material Class	p_{syst}	p_{size}	p_{rec}	p_{orient}
1A	0.02	0	0	0
1B	0.02	0	0	0.03
1C	0.02	0	0	0.03
2A	0.02	0	0	0
2B	0.02	0	0	0.03
2C	0.02	0	0	0.03
3A (<20 mm)	0.04	1	0	0
3A (>20 mm, <30 mm)	0.04	0.8	0	0
3A (>30 mm, <40 mm)	0.04	0.6	0	0
3A (>40 mm, <50 mm)	0.04	0.3	0	0
3A (>50 mm)	0.04	0	0	0
3B	0.04	0	0.1	0.4
3C	0.04	0	0.1	0

As described in Section 4.2, the composition of the input varies per run. For all three non-agglomerated material groups, a value is chosen from the normal distribution. A size is assigned to all free particles from a material-specific Weibull distribution (Tab. 4.3). This distribution is based on research on waste particle size distributions performed by Tanguay-Rioux et al. (2020) and adjusted to match the ratios found from sampling. The distribution of the input is based on the data collected in Test E.

Table 4.2: Input parameters per material group.

	Mean	STD
Share of Foils	0.47	0.05
Share of Rigids	0.12	0.03
Share of Non-plastics	0.32	0.10
Share of particles part of stationary agglomerate	0.05	0.02
Grade agglomeration	0.78	0.05

Table 4.3: Weibull distribution parameters to describe the particle size distribution of the feed.

	Scale factor	Shape factor
Foils	11	1.8
Rigid Plastics	9.0	2.5
Non-plastics	6.55	1.1

4.2.3. Calculation Overlap Error

The model is used to calculate the chance of an overlap error. Test E provides data of the chance of being involved in one of the other errors (p_{tot}) for a range of feedrates. However, the contribution of false calls due to overlapping (p_{over}) of particles can not be extracted from this data alone. So, first, the chance of causing an error when fed in a perfect monolayer (p_{mono}) was calculated by combining the errors in the model. Then, p_{over} was calculated using Equation 4.1. It is assumed that the errors are uncorrelated.

$$p_{tot} = p_{mono} + p_{over} - p_{mono} * p_{over} \tag{4.1}$$

4.3. Results and Discussion

4.3.1. Overlap Errors

First, the model was run with the contribution of overlap errors set to zero. In the graph plot in Fig. 4.1, the difference between the model with a monolayer and the experimental results is shown. The feed in the model does contain particles that form a stationary agglomerate and can therefore not be considered a perfect monolayer. By keeping these particle combinations in the feed in the model, it can be compared to the experimental data and additional assumptions can be avoided. The differences are contributed to p_{over}.

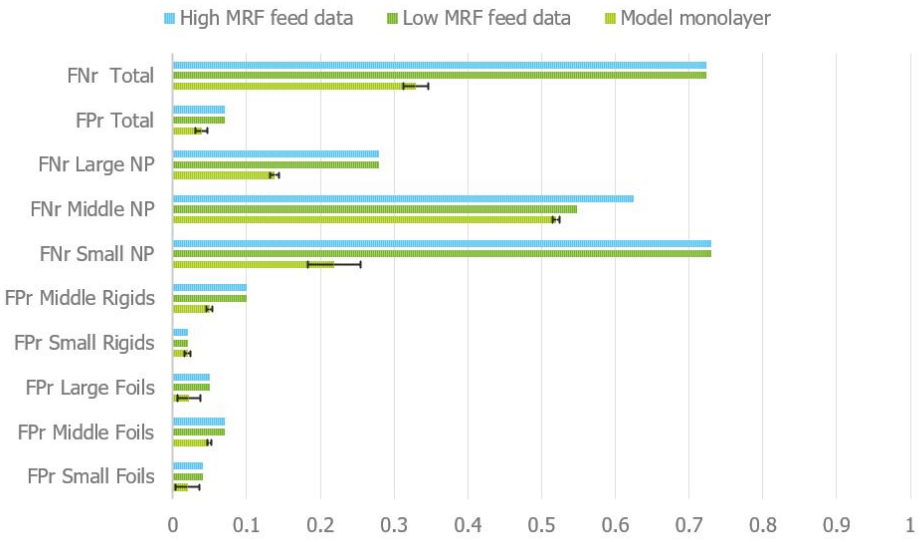

Figure 4.1: Output of the model without overlap v.s. the experimental results.

Using Eq. 4.1, the probabilities p_{over} were determined (Tab. 4.4). The value of p_{over} for small non-plastic particles is high compared to the larger sizes. The relatively high probability can be explained by the choices made in the NIR software. As was seen in Test E, when smaller non-plastics are close to plastic particles, the actuators are not activated. However, it is possible that the results found in Test B (Working Range with Respect to Size Range) can only be applied to clean and pure particles and due to surface contamination of small particles, the number of pixels recognized by the system may not meet the requirements for actuator activation. Lastly, the model accounts for only a p_{size} for which both dimensions are below 50 mm.

4.3.2. Scenarios

The performance indicators were computed for the scenarios and compared to feeding material in a monolayer and the regular feed characteristics (Fig. 4.2). In the model, the share of non-plastics in the NIR feed is calculated using the relations found in Test E. When particles are fed in a monolayer the FPr and FNr are not related to the share of non-plastics. However, the product grade, recovery and mass recovery do depend on the share of non-plastics. Therefore, both input compositions are displayed in the Fig. 4.2. First, it can be concluded that feeding the material in a perfect monolayer

Table 4.4: Values p_{over} per material group.

Material Class	p_{over}
Small Foils	0.020
Middle Foils	0.021
Large Foils	0.030
Small Rigid	0.000
Middle Rigid	0.053
Small Non-plastics	0.654
Middle Non-plastics	0.219
Large Non-plastics	0.165

still only leads to an average grade of 84% at a low share of non-plastics and 75% at a high share. This indicates that a significant part of the feed is outside the working range of the sensor. Apart from the monolayer with the low feedrate composition all scenarios are calculated using the feed composition that is linked to the high feedrate of the MRF because it represents the normal operating conditions.

Tackling the classification and orientation errors leads to the largest improvement of the grade, followed by tackling the stationary agglomeration. Only small differences in the recovery were found as the plastic particles are not likely to cause working range errors and the overlap error is steady within the measured throughput range. Improving the grade does lead to a lower mass recovery since more targeted materials are ejected and do not end up in the product. In scenario 2, the unopened bags were removed from the feed. Since the share of plastics was higher for agglomerated material, removing the agglomeration from the feed results in a lower overall grade.

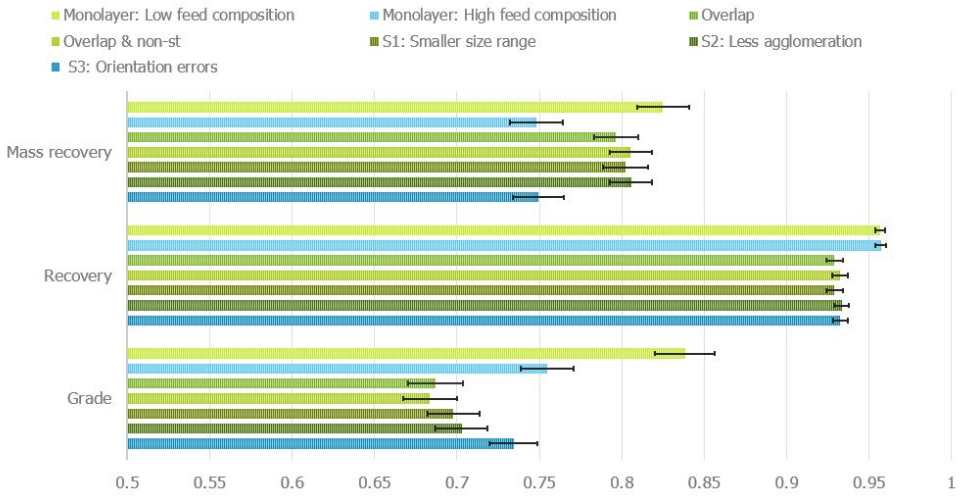

Figure 4.2: Sensor performance of the three scenario's.

In Fig.4.3 the number of particles involved in each type of FC is displayed. In the first scenario 90% of the small particles are removed from the feed. Therefore, the number of systemic FC's is also lower. In all three scenarios. the highest number of particles is involved in an overlap error.

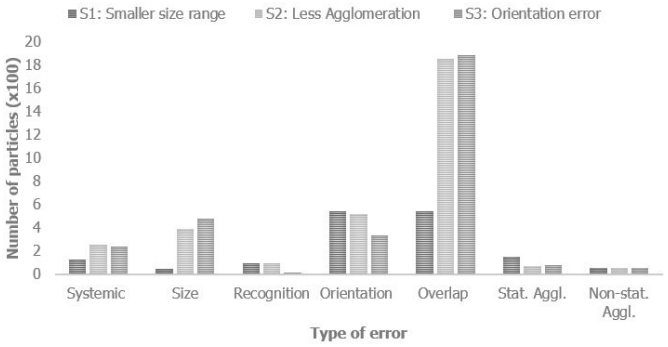

Figure 4.3: Number of errors per type of false call out of total analysed particles.

Key Takeaways Chapter 4

- A statistical model was created to represent the heterogeneity of the feed and performance.
- The probability of an overlap error is larger for non-plastic particles which are to be ejected.
- Three process adjustment scenarios were tested: smaller size range, less agglomerated material and reduction of orientation errors. The latter adjustment is expected to give the most significant results.

5

Discussion

In this study, first, a framework of causes of a FC of an NIR sensor-based sorting system was introduced and applied in a case study in an MRF. Next, a statistical model of the NIR was created to analyse the combination of FC's. This chapter discusses the methodology and the limitations of the experiments and the model. In addition suggestions are made on how the amount of FC's may be reduced.

5.1. Methodology

The applied framework of independent false calls is a new method to analyse sensor sorting performance. Previous research on NIR performance is mainly focused on one or two types of FC's such as recognition or overlapping of particles while other errors are eliminated by feeding in a monolayer or using clean particles. This research provides a starting point for a more elaborate approach of the types of FC's which can provide the means to tackle errors more efficiently.

The framework was applied to an NIR which uses negative sorting to remove contamination from the mixed plastics product. This specific NIR was a suitable system to demonstrate the framework because the feed consisted of a wide range of particle properties which enabled the observation of all types of FC's. An NIR that applies positive sorting and targets, for example, only PET bottles is likely to encounter fewer errors due to working range because the targeted material is relatively homogeneous.

In Test E, the DoE method was applied to determine the probability of an overlap error in relation to the feedrate and feed composition. The feed of the NIR could only be adjusted by adjusting the MRF feedrate. Therefore, the regression analysis was performed in two steps to determine if the feed of the NIR could be controlled as expected. Statistical significant relations between the input factors and the responses were found. However, this approach may not be able to control all variables that influence the FC's. The average weight of non-plastic particles, for example, is higher at a higher feed rate (Appendix B). This could be due to a better performance of the ballistic separator. An increase in weight might lead to an increase in orientation errors because particles become too heavy to be blown over the splitter. It is therefore unknown if the increase of the FNr is entirely due to the higher throughput.

The Monte Carlo analysis allows for the evaluation of waste with a changing feed composition. The standard deviation of the composition was determined using the variation of the centre points in Test E. However, at a higher feed rate the variations in the composition may be larger.

5.2. Limitations

5.2.1. Experiments

In Section 3.2.1 it was determined that a sample should consist of at least 25 particles that are targeted by the sampling analysis to keep the relative sampling error below 20%. This requirement was not met for the large size fraction because of the low occurrence of large particles in the NIR feed. To reduce the sampling error to 20% would require large sample sizes and thus limit the number of samples that could be sorted within the available time. Due to the low occurrence, the influence of the sampling of this category on the total sampling error remains low.

The orientation errors and recognition errors were analysed using samples of more than 100 particles for both non-plastics and plastics. However, the analysed samples are just a snapshot of the feed composition and should be used as an indication of the probability of orientation and recognition errors. Since it is not feasible to sample the entire feed at high frequency, a balance needs to be found.

5.2.2. Statistical Model

The grade, recovery and mass recovery depend on the share of non-plastic particles in the NIR feed and the FPr and FNr. Since the feed composition may change over time, the values are an indication of the possible grades. However, the scenarios can be compared to determine the most effective strategy to reduce FC's.

The error probabilities were determined for this specific NIR. To apply the statistical model to another NIR or for a significant change of the feed characteristics, part of the error probabilities should be redetermined. Table 5.1 states whether the probabilities can still be applied when the feed characteristics are changed. As can be expected, it depends on the type of adjustment. For example, the feeding mechanism could be changed by decreasing the belt speed. This leads to a longer frame time which might improve the recognition of all particles including smaller ones. When the conveyor belt is replaced by a chute, the probability of a systemic error should also be reevaluated. A significant change in feed composition due to for example the addition of a preprocessing step requires the calibration of recognition, orientation and overlap errors.

Table 5.1: Applicability of FC probabilities with altered feed characteristics.

Type of False Call	**Feed rate**	**Feed composition**	**Feeding mechanism**
Systemic	Yes	Yes	Depends on alteration
Size	Yes	Yes	Depends on alteration
Recognition	Yes	No	Depends on alteration
Orientation	Yes	No	No
Overlap	Only if feed < 50% or >100% of MRF feed	No	No

5.3. Application of Results for Process Improvements

The correct ejection of particles fed in a perfect monolayer depends on the NIR sensor settings, such as the belt speed and splitter roll height and distance. These settings are determined by the trajectory of ejected and dropped particles. Again, the range of particle properties is essential. When heavy particles are to be ejected, high air pressure and a low splitter height are required, but this may cause lighter particles to hit the back of the eject box and bounce back. Also, a small range of particle properties makes it easier to adjust the belt speed to prevent the relative movement of 3D particles or the floating of foils. Therefore, the processing steps preceding an NIR should be designed and operated in a way that provides the smallest range of particle properties with the purpose that the feeding mechanism

can be optimized.

The results of this research can be used to identify possibilities for process improvement. Next, a few suggestions for this specific NIR are summed up. Due to the limited time available and the investment that is required to make the adjustments, they were not tested on-site.

Narrow size distribution: The recommended ratio between the smallest and the largest particle is 1:3 to 1:4 (Pretz, 2006). Since the NIR feed currently exceeds this ratio and also contains particles that are out of working range in relation to size, the addition of a sieving step is recommended. The statistical model has shown that removing 90% of the smaller particles slightly improves the grade compared to the current situation because the non-plastic particles are smaller in size than the plastic particles. This indicates that, relatively, more non-plastic particles can be removed. The model does not account for the possible decrease in overlap errors when small particles are removed, which may further improve the grade.

Figure 5.1: Deposition of material on the acceleration belt.

Feeding mechanism: The NIR sensor system is currently fed by two chutes, resulting in two peaks with high occupancy density on the belt. Both of the chutes deposit material from the two identical ballistic separators above. However, the chute on the left (Fig. 5.1) also receives a smaller size fraction from another ballistic separator and is fed from the side instead of the top. This leads to a higher occupancy rate on this side. In addition, video recordings show that part of the particles coming from the right chute hit the sidewall which is placed under a small angle. The particles, therefore, bounce off to the left (white arrow). Additional video analysis is needed to determine the contribution of this movement to the unbalanced particle distribution on the belt.

Fluctuations: In Table 5.2, the list of causes of fluctuations is extended based on on-site observations. Earlier research has shown that fluctuations in the NIR feed may reduce the product grade.

Table 5.2: Overview of causes of fluctuations of the feedrate. Completed with on-site observations.

Location	Fluctuation	Cause	Duration	Frequency	Proposed solution
Wheel loader	Discontinuous feeding of shredder	Discontinues feeding with wheel loader.	Mid term	Irregular	Smart control, instructions wheel loader
Shredder	Bridging	Large particles form bridges in the shredder, making it appear full, influencing the automatic feeding.	Short term to mid term	Irregular	Analysing flow data and machine data.
	Reversing intervals	Shredder settings	Short term	30 sec	-
	Reduced processing rate shredder	Large, thick walled objects are difficult to shred and may block the shredder.	Short term to mid term	Irregular	-
Drum sieve	Fluctuation output	Rotation.	Short term	One drum rotation	Other type of sieve.
	Braid formation	Large foils and wires form braids in the drum sieve.	Short term	Irregular	Regular maintenance intervals shredder. Iron separation before the drum sieve. Other type of sieve.
Input Materials	Heterogeneous input	Large particles.	Short term	Irregular	-
		Residence time of material, municipality, seasonal fluctuations.	Long term	Irregular	-
Windsifters	Blockage	Clustered materials block the suction of air and materials are not removed	Short term to mid term	Irregular	
Chutes	Blockage	After blockage of a chute, all materials are deposited onto the belt in one go	Short term	Irregular	
Conveyor belt	Braid formation	Material gets stuck behind sharp edges.	Mid term	Irregular	Remove sharp edges.
Eddy current and Windsifters	Reduced sorting performance	After an emergency stop, the machines need time to start. If materials are still present in the system, they will not be removed from the main flow. Leading to an increase of flow for part of the process.	Short term to mid term	Irregular	Delay the start of the conveyor belt system after an emergency stop until all machines are ready.

6

Conclusion and Recommendations

6.1. Conclusions

To answer the main research question first the sub-research questions are revisited.

Sub research questions

What is the working range of the NIR?
The working range of an NIR sensor sorting system is the range of particle properties that the system can correctly recognise and eject when targeted. Particle size, shape, density and material type can restrain proper processing. It was found that for the analysed NIR, particles with a dimension below 2 cm cannot be ejected. Starting from 2 cm, the chance of correct classification increases with the particle size. The working range also depends on the database. Due to the wide range of non-plastic particles, not all materials are part of the database. However, an all-encompassing database will not solve all recognition errors. Medical objects, for example, are made of plastics and therefore not ejected, but are unwanted in the mixed plastics product. In addition, the NIR requires monolayer feeding.

What is the relation between each type of false call and feed characteristics (the average feed composition, average feedrate and the feeding mechanism)?
Working range errors are related to the particle properties and therefore also related to the feed composition. It was hypothesised that the chance of whether a false call is made, also depends on the feeding mechanism. For example, a lower belt speed may result in less relative movement to the belt. However, in the experiments performed during this research the feeding mechanism was kept constant.

In literature, it is concluded that the number of false calls related to the overlapping of material depends on all three feed characteristics. In this research, a relation was found between the feedrate and the True Positive rate (FNr); at a higher feedrate the share of non-plastics that are ejected decreases. No statistical relevant relation was found between the feedrate and the False Positives (FP) for the analysed feedrate range. However, there is a difference between the number of FP's when feeding in a monolayer compared to regular feeding. Indicating that for the analysed throughput range, around 8% of the plastics are lost in the eject fraction due to overlap or proximity of particles.

Systemic errors are the only type of false call that is not related to the feed characteristics.

What is the effect of short- and midterm fluctuations of the feed characteristics on the performance?

Short-term feedrate fluctuations are mainly caused by the non-stationary agglomeration of material at this site. However, the number of particles involved in non-stationary agglomeration is relatively low in the current feed. In addition, the grade of the agglomerate is around 70%. Therefore, non-stationary agglomeration only significantly affects the sorting performance when the average product grade is higher.

The results found while answering the sub research questions contribute to the conclusion of the main research question:

To what extent do feedrate, feeding mechanisms and feed composition influence the type and number of false calls in sensor sorting systems and what are ways to control these false calls?

In this research, a framework consisting of five types of relevant false calls was used to analyse the sorting performance of a chosen NIR. The influence of the feed characteristics on the total number of false calls and the ratio between the types of errors varies per NIR.

This research shows that to significantly improve the sorting performance, all feed characteristics need to be optimised. The model of the analysed NIR demonstrates that even if the material is fed in a perfect monolayer the expected grade is 85%. A first step may be to optimise the feed composition based on the working range. Process adjustments like an additional sieving step can narrow the range of particle characteristics and improve the sorting performance.

At the same time, the feeding mechanism can be improved to optimise the distribution of the material on the belt and decrease overlap errors. If the feedrate is kept within the ranges applied in this research, the average p_{over} of medium sized non-plastics will remain around 0.22. Lastly, the reduction of fluctuations decreases underperformance due to on one side overloading and unused potential on the other side.

Analysing the NIR performance by looking into the contribution of the types of FC's can be a useful tool to optimize the sorting results. In the industry, a heterogeneous material flow is fed to the NIR. The preceding processing steps should be optimised and maintained properly with the result that they can be used to their full potential. The NIR's are currently the most advanced technology on-site that aims to produce valuable high-grade materials. The preceding process steps should therefore be used to create a feed within the working ranges of the NIR with an as small as possible range of particle properties.

The steps applied in this research can help to determine if the particle characteristics are suited for the used NIR or if controlling the feedrate should be the main focus. Using NIR's to their full potential will contribute to higher grade sorting products and therefore to better recycling.

6.2. Recommendations

6.2.1. Experimental Improvements

- The quality of a product not only depends on the amount of contamination and on the type of contamination. To create high-quality products, additional tests can be conducted to determine the type of error related to a specific group of contaminants, such as PVC, to target the FC's of this group more efficiently.
- In this research square particles with a size up to 50 mm were analysed to determine the working range. The TPr of particles of 50 mm is only 65%. To determine a cut off value particle sizes in the range of 50 mm to 150 mm should be tested because particles with a size of 150 mm are known to have a TPr of 96% (Test A). It is recommended to use larger batches of clean flakes to determine the size error and systemic error instead of performing multiple runs to reduce the potential influence of adhering dirt.

- Plastic packaging has a low density compared to the materials sorted in other industries using an NIR. Due to the low particle weight and high conveyor belt speed, particles are not immediately pulled along by the conveyor belt. It was observed that foils often linger until they are carried along by another particle. Looking into the interaction between particles on the conveyor belt may provide more insights into the chances of overlap.

6.2.2. Statistical Model Improvement

The model developed in this research is a statistical model with parameters based on observations and sampling. Such a model does not include all possible interactions and changes in the feed. More empirical and theoretical research is needed to describe the influence of all feed characteristics on the sorting performance. Some suggestions are summed up below.

- In the current model, the p_{over} is a function of the MRF feedrate and the position of the blow valves of the windsifter. However, the overlap is also known to depend on the global shape (2D or 3D) and the detailed shape of the particles. By gathering more information on the particle characteristics of non-plastic particles and the influence of the share of rigid materials on the overlap error, the model can be improved to approach industrial sorting more closer. The same goes for small particles. When creating a statistical model to determine the p_{over}, the influence of the processing algorithm should also be taken into account. Because the decision to eject or drop, for example, a combination of a small non-target particle on top of a larger targeted particle depends on the algorithm settings.
- An orientation error can be caused by different particle characteristics in combination with the feeding mechanism: The inability of a particle to lay still, high density or an unfavourable side which prevents recognition, amongst others. By further looking into the causes of orientation errors it can be determined what share can be prevented by for example changing the feeding mechanism. Access to the sensor sorting software and data is needed to make a distinction between these errors.
- Apart from the orientation and recognition errors, all probabilities are assumed to be independent of each other. However, particles with orientation errors might also have a high probability of being involved in overlap errors.
- In this research, the statistical model is not verified using a independent data set. It is recommended to compare the model output to new experimental results of the grade and recovery.

Bibliography

Al-Salem, S., Lettieri, P., & Baeyens, J.. (2009). Recycling and recovery routes of plastic solid waste: A review. *Waste Management*. 29(10), 2625–2643. https://doi.org/10.1016/j.wasman.2009.06.004.

Andrady, A. L. & Neal, M. A.. (2009). Applications and societal benefits of plastics. *Philosophical transactions of the Royal Society of London*. https://doi.org/10.1098/rstb.2008.0304.

Bakker, M. Lecture notes of CIE4710: Material seperation in waste processing, TU Delft. (June 2020).

Brouwer, M., van Velzen, E. T., Ragaert, K., & ten Klooster, R.. (2020). Technical limits in circularity for plastic packages. *Sustainability*. 12. https://doi.org/10.3390/su122310021.

Bukovec, M., Špiclin Ž., Pernuš, F., & Likar, B.. (2007). Automated visual inspection of imprinted pharmaceutical tablets. *Measurement Science and Technology*. 18(9). https://doi.org/10.1088/0957-0233/18/9/023.

Chen, X., Kroell, N., Wickel, J., & Feil, A.. (2021). Determining the composition of post-consumer flexible multilayer plastic packaging with near-infrared spectroscopy. *Waste Management*. 123, 33–41. https://doi.org/10.1016/j.wasman.2021.01.015.

Curtis, A., Küppers, B., Möllnitz, S., Khodier, K., & Sarc, R.. (2021). Real time material flow monitoring in mechanical waste processing and the relevance of fluctuations. *Waste Management*. 120, 687–697. https://doi.org/10.1016/j.wasman.2020.10.037.

De Tandt, E., Demuytere, C., Van Asbroeck, E., Moerman, H., Mys, N., Vyncke, G., Delva, L., Vermeulen, A., Ragaert, P., De Meester, S., & Ragaert, K.. (2021). A recyclers perspective on the implications of reach and food contact material (fcm) regulations for the mechanical recycling of fcm plastics. *Waste Management*. 119, 315–329. https://doi.org/10.1016/j.wasman.2020.10.012.

Ellen Macarthur Foundation. (2016). The new plastics economy: Rethinking the future of plastics. `http://www.ellenmacarthurfoundation.org/publications`.

European Commission. (2019). A new circular economy action plan. `https://eur-lex.europa.eu/legal-content/EN/TXT/?qid=1583933814386&uri=COM:2020:98:FIN`.

Feil, A., van Velzen, E. T., Jansen, M., Vitz, P., Go, N., & Pretz, T.. (2016). Technical assessment of processing plants as exemplified by the sorting of beverage cartons from lightweight packaging wastes. *Waste Management*. 48, 95–105. https://doi.org/10.1016/j.wasman.2015.10.023.

Feil, A., Pretz, T., Vitz, P., & van Velzen, E. U. T.. (2017). A methodical approach for the assessment of waste sorting plants. *Waste Management & Research*. 35(2), 147–154. https://doi.org/10.1177/0734242X16683270.

Feil, A., Coskun, E., Bosling, M., Kaufeld, S., & Pretz, T.. (2019). Improvement of the recycling of plastics in lightweight packaging treatment plants by a process control concept. *Waste Management & Research*. 37. https://doi.org/10.1177/0734242X19826372.

Gülcan, E.. (2020). A novel approach for sensor based sorting performance determination. *Minerals Engineering*. 146. https://doi.org/10.1016/j.mineng.2019.106130.

Gülcan, E. & Gülsoy, Ã.. (2017). Performance evaluation of optical sorting in mineral processing: A case study with quartz, magnesite, hematite, lignite, copper and gold ores. *International Journal of Mineral Processing*. 169, 129–141. https://doi.org/10.1016/j.minpro.2017.11.007.

Gundupalli, S., Hait, S., & Thakur, A.. (2017). A review on automated sorting of source-separated municipal solid waste for recycling. *Waste Management*. 60, 56–74. https://doi.org/10.1016/j.wasman.2016.09.015.

Hahladakis, J. & Iacovidou, E.. (2018). Closing the loop on plastic packaging materials: What is quality and how does it affect their circularity? *Science of The Total Environment*. 630. https://doi.org/10.1016/j.scitotenv.2018.02.330.

Hahladakis, J., Velis, C., Weber, R., Iacovidou, E., & Purnell, P.. (2018). An overview of chemical additives present in plastics: Migration, release, fate and environmental impact during their use, disposal and recycling. *Journal of Hazardous Materials*. 344, 179–199. https://doi.org/10.1016/j.jhazmat.2017.10.014.

Jambeck, J. R., Geyer, R., Wilcox, C., Siegler, T., Perryman, M., Anthony, A. A., Narayan, R., & Law, K.. (2015). Plastic waste inputs from land into the ocean. *Science*. 347(6223), 768–771. https://doi.org/10.1126/science.1260352.

Jansen, M., van Velzen, E. T., & Pretz, T. Handbook for the sorting of plastic packaging waste concentrates. Technical report. Wageningen UR Food & Biobased Research. (2015).

Julius, J. & Pretz, T. *Separating Pro-Environment Technologies for Waste Treatment, Soil and Sediments Remediation*. Bentham Books. (2012).

Kandlbauer, L., Khodier, K., Ninevski, D., & Sarc, R.. (2021). Sensor-based particle size determination of shredded mixed commercial waste based on two-dimensional images. *Waste Management*. 120, 784–794. https://doi.org/10.1016/j.wasman.2020.11.003.

Khodier, K., Feyerer, C., Möllnitz, S., Curtis, A., & Sarc, R.. (2021). Efficient derivation of significant results from mechanical processing experiments with mixed solid waste: Coarse-shredding of commercial waste. *Waste Management*. 121, 164–174. https://doi.org/10.1016/j.wasman.2020.12.015.

Kleinhans, K., Hallemans, M., Huysveld, S., Thomassen, G., Ragaert, K., Geem, K. V., Roosen, M., Mys, N., Dewulf, J., & Meester, S. D.. (2021). Development and application of a predictive modelling approach for household packaging waste flows in sorting facilities. *Waste Management*. 120, 290–302. ISSN 0956-053X. https://doi.org/10.1016/j.wasman.2020.11.056.

Küppers, B., Schögl, S., Oreski, G., Pomberger, R., & Vollprecht, D.. (2019). Influence of surface roughness and surface moisture of plastics on sensor-based sorting in the near infrared range. *Waste Management & Research*. 37(8), 843âĂŞ850. https://doi.org/10.1177/0734242x19855433.

Küppers, B., Seidler, I., Koinig, G., Pomberger, R., & Vollprecht, D.. (2020). Influence of throughput rate and input composition on sensor-based sorting efficiency. *Detritus*. https://doi.org/10.31025/2611-4135/2020.13906.

Küppers, B., Schlögl, S., Friedrich, K., Lederle, L., Pichler, C., Freil, J., Pomberger, R., & Vollprecht, D.. (2021). Influence of material alterations and machine impairment on throughput related sensor-based sorting performance. *Waste Management & Research*. 39(1), 122–129. https://doi.org/10.1177/0734242X20936745.

Lebersorger, S. & Schneider, F.. (2011). Discussion on the methodology for determining food waste in household waste composition studies. *Waste Management*. 31(9), 1924–1933. https://doi.org/10.1016/j.wasman.2011.05.023.

Lebreton, L. & Andrady, A.. (2019). Future scenarios of global plastic waste generation and disposal. *Palgrave Commun*. https://doi.org/10.1057/s41599-018-0212-7.

Luijsterburg, B. & Goossens, H.. (2014). Assessment of plastic packaging waste: Material origin, methods, properties. *Resources, Conservation and Recycling*. 85, 88–97. https://doi.org/10.1016/j.resconrec.2013.10.010.

McKinnon, D., Punkkinen, H., Wahlström, M., Bakas, M., Herczeg, I., Vea, E., Busch, N., Christensen, L., Christensen, C., Damgaard, C., & Milios, L.. (2018). Plastic waste markets: Overcoming barriers to better resource utilisation. https://doi.org/10.6027/TN2018-525.

Milieu Centraal. Afval scheiden: cijfers en kilo's. (2018). `https://www.milieucentraal.nl/minder-afval/afval-scheiden/afval-scheiden-cijfers-en-kilo-s/`.

Nihot Airconomy. Wss windshifter. (n.d.). `https://nihot.nl/products/wss-windshifter/`.

Ooms, D., Palm, R., Leemans, V., & Destain, M.. (2010). A sorting optimization curve with quality and yield requirements. *Pattern Recognition Letters*. 31(9), 983–990. https://doi.org/10.1016/j.patrec.2009.12.015.

Park, C.-H., Jeon, H.-S., & Park, J.-K.. (2007). Pvc removal from mixed plastics by triboelectrostatic separation. *Journal of Hazardous Materials*. 144(1), 470–476. https://doi.org/10.1016/j.jhazmat.2006.10.060.

Pascoe, R., Udoudo, O., & Glass, H.. (2010). Efficiency of automated sorter performance based on particle proximity information. *Minerals Engineering*. 23(10), 806–812. https://doi.org/10.1016/j.mineng.2010.05.021.

Plastics Europe. (2020). Plastics - the facts 2019. `https://www.plasticseurope.org/nl/resources/publications/1804-plastics-facts-2019`.

Pretz, T. The state of the art in sensor-based sorting. (2006). Conference conducted at the meeting of Enhanced Landfill Mining. Mechelen, Belgium.

Rozenstein, O., Puckrin, E., & Adamowski, J.. (2017). Development of a new approach based on mid-wave infrared spectroscopy for post-consumer black plastic waste sorting in the recycling industry. *Waste Management*. 68, 38–44. https://doi.org/10.1016/j.wasman.2017.07.023.

Rubel, H., Follete, C., zum Felde, A. M., Appathurai, S., Diaz, M. B., & Jung, U. A circular solution to plastic waste. (2019). `https://www.bcg.com/publications/2019/plastic-waste-circular-solution`.

Sarc, R., Curtis, A., Kandlbauer, L., Khodier, K., Lorber, K., & Pomberger, R.. (2019). Digitalisation and intelligent robotics in value chain of circular economy oriented waste management: A review. *Waste Management*. 95, 476–492. https://doi.org/10.1016/j.wasman.2019.06.035.

Shamsuyeva, M. & Endres, H.. (2021). Plastics in the context of the circular economy and sustainable plastics recycling: Comprehensive review on research development, standardization and market. *Composites Part C: Open Access*. 6. https://doi.org/10.1016/j.jcomc.2021.100168.

Shen, L. & Worrell, E. Chapter 13 - plastic recycling. In Worrell, E. & Reuter, M. A., editors, *Handbook of Recycling*. pages 179–190. Elsevier. Boston. (2014). https://doi.org/10.1016/B978-0-12-396459-5.00013-1.

Shen, M., Huang, W., Chen, M., Song, B., Zeng, G., & Zhang, Y.. (2020). (micro)plastic crisis: Un-ignorable contribution to global greenhouse gas emissions and climate change. *Journal of Cleaner Production*. 254. https://doi.org/10.1016/j.jclepro.2020.120138.

Sympatec GmbH. Particle shape and shape descriptors. (n.d.). https://www.sympatec.com/en/particle-measurement/glossary/particle-shape/.

Tanguay-Rioux, F., Legros, R., & Spreutels, L.. (2020). Particle size analysis of municipal solid waste for treatment process modeling. *Waste Management & Research*. 38(7), 783–791. 10.1177/0734242X20918007.

Tatzer, P., Wolf, M., & Panner, T.. (2005). Industrial application for inline material sorting using hyperspectral imaging in the nir range. *Real-Time Imaging*. 11(2), 99–107. https://doi.org/10.1016/j.rti.2005.04.003.

Thiounn, T. & Smith, R.. (2020). Advances and approaches for chemical recycling of plastic waste. *Journal of Polymer Science*. 58, p.1347–1364. https://doi.org/10.1002/pol.20190261.

Ügdüler, S., Van Geem, K. M., Roosen, M., Delbeke, E. I., & De Meester, S.. (2020). Challenges and opportunities of solvent-based additive extraction methods for plastic recycling. *Waste Management*. 104, 148–182. https://doi.org/10.1016/j.wasman.2020.01.003.

Wen, P., Lohlefink, G., & Rem, P.. (2021). Non-overlapping coverage in random feeding. *Powder Technology*. 385, 50–59. https://doi.org/10.1016/j.powtec.2021.02.068.

Wotruba, H. Plenary lecture:sensor sorting technology - is the minerals industry missing a chance?. (2006). RWTH Aachen University, Department of Mineral Processing, Aachen, Germany.

Zerbini, P. E.. (2006). Emerging technologies for non-destructive quality evaluation of fruit. *Journal of Fruit and Ornamental Plant Research*. 14.

Zheng, J. & Suh, S.. (2019). Strategies to reduce the global carbon footprint of plastics. *Nature Climate Change*. https://doi.org/10.1038/s41558-019-0459-z.

A

Data Test C

Table A.1: Number of False Positives per individual particle after 3 batch runs. Batch Material: True Positives

Number of FN/runs	Number of particles [n]	Share of total particles
0/3	33	56%
1/3	12	20%
2/3	11	19%
3/3	9	15%
3/3 (Classification error)	0	0%
Total	65	100%

Table A.2: Number of False Positives per individual particle after 3 batch runs. Batch Material: True Negatives

Number of FP/runs	Number of particles [n]	Share of total particles
0/3	123	90%
1/3	7	5%
2/3	4	3%
3/3	3	2%
3/3 (Classification error)	0	0%
Total	137	100%

Table A.3: Number of False Positives per individual particle after 3 batch runs. Batch Material: False Positives

Number of FP/runs	Number of particles [n]	Share of total particles
0/3	81	84%
1/3	11	11%
2/3	4	4%
3/3	1	1%
3/3 (Classification error)	0	0%
Total	97	100%

B

Data Test E

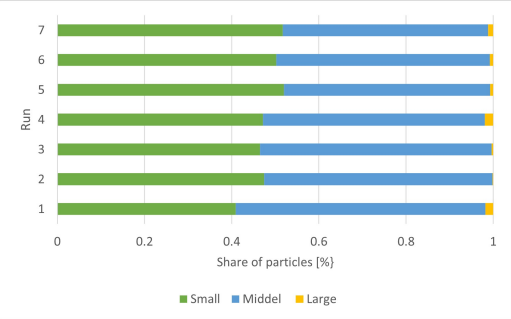

(a) Input size fractions particles.

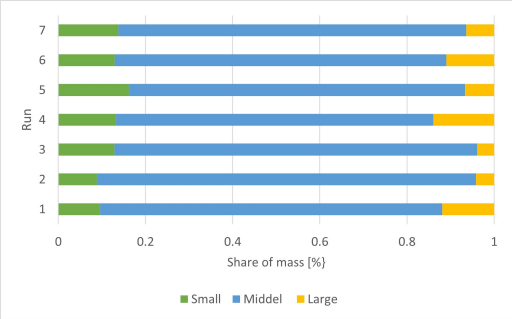

(b) Input composition mass.

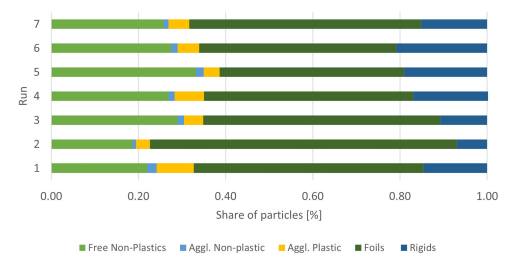

(c) Input composition particles.

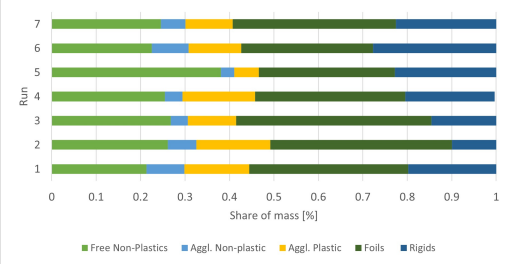

(d) Input composition mass.

Figure B.1: Average input composition of each run

Table B.1: Results performance indicators per run

	Low, Open	Low, Closed	High, Open	High, Closed	Centerpoint 1	Centerpoint 2	Centerpoint 3
Feedrate Mass	0.74	0.94	1.18	2.03	1.28	1.10	0.96
Feedrate Particles	136	178	206	334	212	190	186
Feedrate NIR	4500	5000	5900	6300	5300	5200	5500
FPr particles	6%	0.06	0.08	0.04	0.06	0.11	0.06
FPr mass	0.08	0.09	0.08	0.03	0.05	0.09	0.06
TPr Particles	0.34	0.21	0.32	0.16	0.29	0.34	0.28
TPr Mass	0.40	0.33	0.38	0.20	0.34	0.33	0.30
Purity particles	85%	73%	72%	73%	81%	78%	79%
Purity mass	76%	75%	68%	73%	77%	77%	77%
Yield particles	94%	94%	92%	96%	95%	91%	94%
Yield mass	93%	90%	93%	97%	95%	92%	94%
Recovery particles	88%	89%	84%	93%	89%	84%	88%
Recovery mass	83%	83%	80%	92%	87%	80%	87%
FPr Small Foils	0.03	0.05	0.06	0.04	0.02	0.10	0.02
FPr Middle Foils	0.08	0.07	0.10	0.05	0.07	0.09	0.09
FPr Small Rigids	0.04	0.03	0.04	0.03	0.06	0.06	0.07
FPr Middle Rigids	0.08	0.15	0.11	0.03	0.10	0.14	0.07
TPr Small Non-Plastics	0.29	0.16	0.28	0.14	0.24	0.34	0.24
TPr Middle Non-Plastics	0.38	0.36	0.41	0.21	0.39	0.36	0.41

Table B.2: Average particle mass of medium size fraction non-plastics

	Non-plastic particles in product			Non-plastic particles in residue		
Run	**Total Mass [kg]**	**Nr of particles**	**Avg particle mass**	**Total Mass [kg]**	**Nr of particles**	**Avg particle mass**
Center point	0.28	25.00	0.011	0.40	30.00	0.013
Center point	0.44	28.00	0.016	0.64	48.00	0.013
Low feed, open valves	0.30	25.00	0.012	0.36	37.00	0.010
Low feed, open valves	0.38	31.00	0.012	0.38	25.00	0.015
Low feed, closed valves	0.44	31.00	0.014	1.16	71.00	0.016
Low feed, closed valves	0.40	27.00	0.015	0.42	28.00	0.015
Center point	0.30	26.00	0.012	0.34	21.00	0.016
Center point	0.42	25.00	0.017	0.46	34.00	0.014
High feed, open valves	0.64	23.00	0.028	0.42	29.00	0.014
High feed, open valves	0.44	27.00	0.016	0.78	48.00	0.016
High feed, closed valves	0.54	25.00	0.022	0.26	21.00	0.012
High feed, closed valves	0.38	25.00	0.015	0.68	36.00	0.019
Center point	0.60	28.00	0.021	0.54	33.00	0.016
Center point	0.20	12.00	0.017	0.54	33.00	0.016

Table B.3: Average particle mass non-plastics for different MRF feedrates

	Non-plastic particles in product	**Non-plastic particles in residue**
Center point	0.016	0.015
Low feed	0.013	0.014
High feed	0.020	0.016

C

Monte Carlo Runs

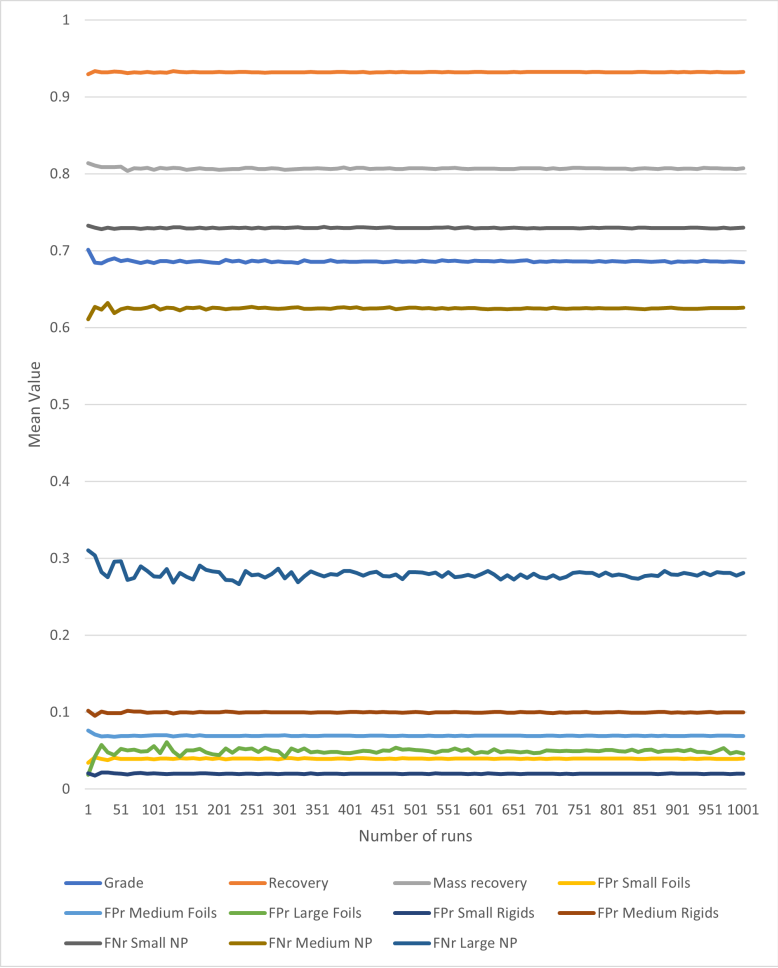

Figure C.1: Mean value of results versus the number of runs

D

Matlab File

Matlab Code

```
clear all
close all


% Scenario 0.0 = Stationary agglomerate in feed, no free particle overlap and non-stationary agglomerate
% Scenario 0.1 = Overlap, no non-stationary agglomerate
% Scenario 0.2 = Overlap and non-stationary agglomerate
% Scenario 1 = Narrow Size distribution
% Scenario 2 = Recuding stationary agglomeration
% Scenario 3 = Reducing recognition and orientation errors

Scenario = 4;

tic

%% Input parameters

nT = 10000;                         % Number of particles

ThroughputMRF = 100;                % Feed of material recovery facility [% of maximal throughput]
Wind = 0;                           % Closing of the blow valve of the windsifter (percentage closed)

FeedP = 58.5 + 1.4 * ThroughputMRF - 0.440 * Wind + 0.0172 * Wind * ThroughputMRF;                    % NIR feed [particles per second]

Time = nT/FeedP;                    % Running time [sec]

meanfoils = 1.0146 - 0.00578 * ThroughputMRF - 0.003546 * Wind + 0.000039 *
```

```
    ThroughputMRF * Wind;  %Average share of foils of free particles
28 meanrigid = -0.0165 + 0.002338 * ThroughputMRF;          %Average share of rigid
     plastics of free particles
29 meanwaste = 0.0325 + 0.003242 * ThroughputMRF + 0.002933 * Wind -3.5*10^-5 *
    ThroughputMRF * Wind;  %Average share of non-plastics of free particles
30 meanSA = 0.05;           %Average share of stationary agglomerate in the input [
    particles/particles]
31 meanSAplastics = 0.78;      % Share of plasticparticles in stationary
    agglomerate
32
33 STDfoils = 0.029;
34 STDrigid = 0.015;
35 STDwaste = 0.015;
36 STDSA = 0.02;
37 STDSAplastics = 0.05;       % STD of share of plastics in stationary agglomerate
38
39 if Scenario == 3
40     STDSAplastics = 0.025;
41     meanSAplastics = 0.90;
42 end
43
44 ShareNSAplastics = 0.71;     % STD of share of plastics in stationary
    agglomerate
45
46 TimeNStAggl = 5;            % Time between non-stationary agglomeration [sec]
47 PNStAggl = 20;               % Particles per non-stationary agglomeration
48
49
50 %% Average particle mass per material class
51
52 MassSF = 0.0007;
53 MassMF = 0.0054;
54 MassLF = 0.0347;
55
56 MassSR = 0.0034;
57 MassMR = 0.0117;
58
59 MassSW = 0.00165;
60 MassMW = 0.0164;
61 MassLW = 0.147;
62
63 MassSAP = 0.013;
64 MassSAW = 0.021;
65
66
67 %% Parameters: Error p-values
68
69 psystw = 0.04;           % systemic errors plastics
70 psystp = 0.02;           % systemic errors non-plastics
71
```

```
72  p1size = 0.3;           % Size errors: Size between 2 cm and 3 cm
73  p2size = 0.6;           % Size errors: Size between 3 cm and 4 cm
74  p3size = 0.8;           % Size errors: Size between 4 cm and 5 cm
75
76  precw = 0.1;          % deterministic uniqueness/working range errors non-
        plastics
77  precp = 0.00;         % deterministic uniqueness/working range errors plastic
78
79  porientw = 0.40 / (1 - precw);          % orientation error non-plastics
80  porientp = 0.03 / (1 - precp) ;         % orientation error plastics
81
82  pagglw = 0.95;                            % Error agglomerated non-plastics
83  pagglp = 0.02;                            % Error agglomerated plastics
84
85  pOFoilsS = 0.02;
86  pOFoilsM = 0.021;
87  pOFoilsL = 0.03;
88
89  pORigidS = 0.000;
90  pORigidM = 0.053;
91  pORigidL = 0.0 ;
92
93  pOWasteS = 0.654;
94  pOWasteM = 0.219;
95  pOWasteL = 0.165;
96
97  if Scenario == 0
98
99  pOWasteS = 0;
100 pOWasteM = 0;
101 pOWasteL = 0;
102
103 pOFoilsS = 0;
104 pOFoilsM = 0;
105 pOFoilsL = 0;
106
107 pORigidS = 0;
108 pORigidM = 0;
109 pORigidL = 0 ;
110
111 end
112
113 if Scenario == 3
114
115 precw = 0.01;          % deterministic uniqueness/working range errors non-
        plastics
116 precp = 0.00;         % deterministic uniqueness/working range errors plastic
117
118 porientw = 0.20 / (1 - precw);          % orientation error non-plastics
119 porientp = 0.03 / (1 - precp) ;         % orientation error plastics
```

```
120
121 end
122
123
124 %% Start monte carlo runs
125
126 Monte = zeros(1000,20);          %Empty matrix to save results of each run
127
128 for j = 1:1:1000
129 nT = 10000;                      % Number of particles
130
131     %% Feed composition
132
133 ShareFoilsP = normrnd(meanfoils,STDfoils);              % Share of foils of free
        particles, random number from normal distribution
134 ShareRigidP = normrnd(meanrigid,STDrigid);              % Share of rigid of free
        particles, random number from normal distribution
135 ShareWasteP = normrnd(meanwaste,STDwaste);              % Share of non-plastics
        (waste) of free particles, random number from normal distribution
136 ShareStAggl = normrnd(meanSA,STDSA);                   % Share of non-
        plastics (waste) in the input, random number from normal distribution
137
138
139 ShareFoils = (ShareFoilsP/(ShareRigidP + ShareWasteP + ShareFoilsP)) * (1-
        ShareStAggl);              % Share of foils in the input, random number from
         normal distribution
140 ShareRigid = (ShareRigidP/(ShareRigidP + ShareWasteP + ShareFoilsP)) * (1-
        ShareStAggl);          % Share of rigid plastics in the input, random
        number from normal distribution
141 ShareWaste = (ShareWasteP/(ShareRigidP + ShareWasteP + ShareFoilsP)) * (1-
        ShareStAggl);              % Share of non-plastics (waste) in the input,
        random number from normal distribution
142
143
144 ShareAplastics = normrnd(meanSAplastics,STDSAplastics);          % Share of
        plastics in stationary agglomerate, random number from normal distribution
145
146 if ShareAplastics > 1                                  % Share of plastics can not
         be higher than 1
147     ShareAplastics = 1;
148 end
149
150 ShareAwaste = 1 - ShareAplastics;              % Share of non-plastics (waste)
        in agglomerated material, random number from normal distribution
151 ShareStAggl = 1 - ShareFoils - ShareRigid - ShareWaste;        % Share of
        stationary agglomerated material
152
153
154
155 nNSA = floor((Time/TimeNStAggl)) * PNStAggl;        % Total Non-St Agglomarate
```

```
    during one batch
156
157 if Scenario == 0 || Scenario == 0.1
158     nNSA = 0;
159 end
160
161 nA = round(nT * ShareStAggl);          % Number of Agglomerated particles
162 nNA = nT - nA;                         % Number of Free particles (Non-
    Agglomerated)
163
164 nNSAPlastics = round(ShareNSAplastics * nNSA);          % Share of plastics non
    -st agglomerate
165 nNSAWaste = round((1-ShareNSAplastics) * nNSA);             % Share of non-
    plastics in non-st agglomerate
166
167
168 nT = nT + nNSA;                        % Non-stationary Agglomerated particles are
     added to the total amount of particles
169
170
171 % Number of particles per material type
172
173 nFoils = round(ShareFoils * (nNA+nA));
174 nRigids = round(ShareRigid * (nNA+nA));
175 nWaste = round(ShareWaste * (nNA+nA));
176
177 nAPlastics = round(ShareAplastics * nA);              % Number of stationary
    agglomerated plastic particles
178 nAWaste = round(ShareAwaste * nA);                  % Number of stationary
    agglomerated non-plastic particles
179
180
181 % Three matrixes to reduce running time
182
183 P = zeros(nNA,13);                          % Free particles (Non-Agglomeration
    ) matrix
184 PA = zeros(nA,13);                          % Stationary agglomeration matrix
185 PNSA = zeros(nNSA,13);                      % Non- Stationary agglomeration
    matrix
186
187
188 %% Type of material (column 1)
189 % Material types
190
191 % 1 = Foils
192 % 2 = Rigids
193 % 3 = Non-Plastics
194 % 4 = St-Aggl Plastics
195 % 5 = St-Aggl Non-Plastics
196 % 6 = N-St-Aggl Plastics
```

```
197 % 7 = N-St-Aggl Non-Plastics
198
199
200 P(1:nFoils, 1) = 1;
201 P((nFoils + 1):(nFoils + nRigids), 1) = 2;
202 P((nFoils + nRigids + 1):(nFoils + nRigids + nWaste), 1) = 3;
203
204
205 PA(1:(nAPlastics), 1) = 4;
206 PA((nAPlastics + 1):(nAPlastics + nAWaste), 1) = 5;
207
208
209 PNSA(1:(nNSAPlastics), 1) = 6;
210 PNSA((nNSAPlastics + 1):(nNSAPlastics + nNSAWaste), 1) = 7;
211
212
213
214 %% Particle size  (Column 2 & Column 3)
215
216 for i = 1:1:nNA
217     if P(i,1) == 1
218         P(i,2) = wblrnd(11,1.8);
219         P(i,3) = wblrnd(11,1.8);
220
221     end
222
223     if P(i,1) == 2
224         P(i,2) = wblrnd(9.0,2.5);
225         P(i,3) = wblrnd(9.0,2.5);
226
227     end
228
229     if P(i,1) == 3
230         P(i,2) = wblrnd(6.55, 1.1);
231         P(i,3) = wblrnd(6.55, 1.1);
232     end
233
234 end
235
236
237 % Assign particle to size fraction based on the value in column 2 and 3
238 % 1 = Small
239 % 2 = Middle
240 % 3 = Large
241
242 for i = 1:1:nNA
243    if  (P(i,2) < 5 && P(i,3) < 15) || (P(i,2) < 15 && P(i,3) < 5)
244        P(i,12) = 1;
245    end
246    if  (P(i,2) > 5 && P(i,3) <30 && P(i,3)>5) ||(P(i,2) < 30 && P(i,3) > 5 && P
```

```
        (i,2)>5) ||(P(i,2) < 5 && P(i,3) >15) || (P(i,2) > 15 && P(i,3) < 5)
247           P(i,12) =2;
248     end
249     if (P(i,2) > 30 || P(i,3) > 30)
250           P(i,12) = 3;
251     end
252 end
253
254 %% Particle weigth
255
256 %% 1. Systemic Errors (colomn 4)
257
258 for i = 1:1:nNA
259     P(i,4) = rand;                  % Gives all free particles a random number
            between 0 and 1 in column 4
260     if P(i,1) == 3
261         if P(i,4) < psystw          % If random value is < p, the particle is
                sorted incorrectly (1)
262         P(i,4) = 1;
263         else                        % If random value is > p, the particle is
                sorted correctly (0)
264         P(i,4) = 0;
265         end
266
267     else
268         if P(i,4) < psystp
269         P(i,4) = 1;
270         else
271         P(i,4) = 0;
272         end
273     end
274 end
275
276
277
278 %% Working range: Size (column 5)
279
280 for i = 1:1:nNA
281     if P(i,1) == 3
282     if P(i,2)< 2.0 && P(i,3)< 2.0
283         P(i,5)=1;
284     end
285
286     if P(i,2) > 2.0 && P(i,2) < 3.0 && P(i,3) < 3.0
287         P(i,5) = rand;
288         if P(i,5) < plsize
289             P(i,5) = 1;
290         else
291             P(i,5) = 0;
292         end
```

```
293     end
294
295     if P(i,2) > 3.0 && P(i,2) < 4.0 && P(i,3) < 4.0
296         P(i,5) = rand;
297         if P(i,5) < p2size
298             P(i,5) = 1;
299         else
300             P(i,5) = 0;
301         end
302     end
303
304     if P(i,2) > 4.0 && P(i,2) < 5.0 && P(i,3) < 5.0
305         P(i,5) = rand;
306         if P(i,5) < p3size
307             P(i,5) = 1;
308         else
309             P(i,5) = 0;
310         end
311     end
312     end
313 end
314
315 %% Working range: Classification error (column 6)
316
317 for i = 1:1:nNA
318     if P(i,12) == 2 || P(i,12) == 3            % If material is in the Middle
        or Large size fraction
319         P(i,6) = rand;
320         if P(i,1) == 3
321             if P(i,6) < precw
322                 P(i,6) = 1;
323             else
324                 P(i,6) = 0;
325             end
326
327         else
328             if P(i,6) < precp
329                 P(i,6) = 1;
330             else
331                 P(i,6) = 0;
332             end
333         end
334     end
335 end
336
337 %% Orientation (column 7)
338
339
340 for i = 1:1:nNA
341     if P(i,12) == 2
```

```
342         if P(i,6) == 0              % Particle can not have a classification
                error and orientation error at the same time.
343             P(i,7) = rand;
344             if P(i,1) == 3
345                 if P(i,7) < porientw
346                     P(i,7) = 1;
347                 else
348                     P(i,7) = 0;
349                 end
350
351             else
352                 if P(i,7) < porientp
353                     P(i,7) = 1;
354                 else
355                     P(i,7) = 0;
356                 end
357             end
358         end
359     end
360 end
361
362
363
364
365 %% Overlap (colomn 8)
366
367 for i = 1:1:nNA
368         P(i,8) = rand;
369         if P(i,1) == 1
370             if P(i,12) == 1
371                 if P(i,8) < pOFoilsS
372                    P(i,8) = 1;
373                 else
374                    P(i,8) = 0;
375                 end
376
377             elseif P(i,12) == 2
378                 if P(i,8) < pOFoilsM
379                    P(i,8) = 1;
380                 else
381                    P(i,8) = 0;
382                 end
383
384             else
385                 if P(i,8) < pOFoilsL
386                    P(i,8) = 1;
387                 else
388                    P(i,8) = 0;
389                 end
390
```

```
391             end
392         end
393
394          if P(i,1) == 2
395             if P(i,12) == 1
396                 if P(i,8) < pORigidS
397                    P(i,8) = 1;
398                 else
399                    P(i,8) = 0;
400                 end
401
402             elseif P(i,12) == 2
403                 if P(i,8) < pORigidM
404                    P(i,8) = 1;
405                 else
406                    P(i,8) = 0;
407                 end
408
409             else
410                 if P(i,8) < pORigidL
411                    P(i,8) = 1;
412                 else
413                    P(i,8) = 0;
414                 end
415             end
416          end
417
418           if P(i,1) == 3
419             if P(i,12) == 1
420                 if P(i,8) < pOWasteS
421                    P(i,8) = 1;
422                 else
423                    P(i,8) = 0;
424                 end
425
426
427             elseif P(i,12) == 2
428
429                 if P(i,8) < pOWasteM
430                    P(i,8) = 1;
431                 else
432                    P(i,8) = 0;
433                 end
434
435             else
436                 if P(i,8) < pOWasteL
437                    P(i,8) = 1;
438                 else
439                    P(i,8) = 0;
440                 end
```

```
441                 end
442             end
443 end
444
445
446 %% Stationary Agglomeration (colomn 9)
447
448
449 for i = 1:1:nA
450     PA(i,9) = rand;
451     if PA(i,1) == 5
452         if PA(i,9) < pagglw
453             PA(i,9) = 1;
454         else
455             PA(i,9) = 0;
456         end
457
458     else
459         if PA(i,9) < pagglp
460             PA(i,9) = 1;
461         else
462             PA(i,9) = 0;
463         end
464     end
465 end
466
467 PT = [P;PA];
468
469
470
471
472 %% Non-stationary Agglomeration (column 10)
473
474
475 for i = 1:1:nNSA
476     if PNSA(i,1) == 7
477         PNSA(i,10) = 1;
478
479     else
480         PNSA(i,10) = 0;
481     end
482 end
483
484
485 PT = [PT;PNSA];
486
487 if Scenario == 1
488 for i = 1:1:nT
489     if PT(i, 12) == 1
490         PT(i, 12) = rand;
```

```
491             if PT(i,12) < 0.1
492                 PT(i,12) = 1;
493             else PT(i,:) = 0;
494
495             end
496
497         end
498     end
499     end
500
501     nT = size(PT,1);
502
503
504     %% Results
505
506     S=sum(PT(:,4:10),2);  % Sum of all errors
507     PT(:,11) = S;          % Sum of all errors is saved in Column 11
508
509     S_TypeError = sum(PT);  % Sum per type of error
510
511
512     TP = 0;      %Number of True Positives
513     TN = 0;      %Number of True Negatives
514     FN = 0;      %Number of False Negatives
515     FP = 0;      %Number of False Positives
516
517
518     SF = 0;      %Number of Small Foils
519     MF = 0;      %Number of Middle Foils
520     LF = 0;      %Number of Large Foils
521
522
523     TNSF = 0;   %True Negative Rate Small Foils
524     FPSF = 0;
525
526     TNMF = 0;
527     FPMF = 0;
528
529     TNLF = 0;
530     FPLF = 0;
531
532     SR = 0;      % Small Rigids
533     MR = 0;
534     LR = 0;
535
536
537     TNSR = 0;
538     FPSR = 0;
539
540     TNMR = 0;
```

```
FPMR = 0;

TNLR = 0;
FPLR = 0;

SW = 0;      % Small non-plastics (Waste)
MW = 0;
LW = 0;


TPSW = 0;
FNSW = 0;

TPMW = 0;
FNMW = 0;

TPLW = 0;
FNLW = 0;


% Rates

for i = 1:1:(nT)
    if PT(i,1) == 3 || PT(i,1) == 5 || PT(i,1) ==7
        if PT(i,11) == 0
            TP = TP + 1;
        else
            FN = FN + 1;
        end
    else
        if PT(i,11) == 0
            TN = TN + 1;
        else
            FP = FP + 1;
        end
    end
end

%Foils

for i = 1:1:nT
    if PT(i,1) == 1 && P(i,12) == 1
        SF=SF+1;
        PT(i,13) = MassSF;
        if PT(i,11) == 0
            TNSF = TNSF + 1;
        else
            FPSF = FPSF + 1;
        end
    end
```

```
591     if PT(i,1) == 1 && P(i,12) == 2
592         MF = MF + 1;
593         PT(i,13) = MassMF;
594         if PT(i,11) == 0
595             TNMF = TNMF + 1;
596         else
597             FPMF = FPMF + 1;
598         end
599     end
600     if PT(i,1) == 1 && P(i,12) == 3
601         LF = LF +1;
602         PT(i,13) = MassLF;
603         if PT(i,11) == 0
604             TNLF = TNLF + 1;
605         else
606             FPLF = FPLF + 1;
607         end
608     end
609 end
610
611 FPrSF = FPSF/SF;
612 FPrMF = FPMF/MF;
613 FPrLF = FPLF/LF;
614
615 %Rigids
616
617 for i = 1:1:nT
618     if PT(i,1) == 2 && P(i,12) == 1
619         SR=SR+1;
620         PT(i,13) = MassSR;
621         if PT(i,11) == 0
622             TNSR = TNSR + 1;
623         else
624             FPSR = FPSR + 1;
625         end
626     end
627     if PT(i,1) == 2 && P(i,12) == 2
628         MR = MR + 1;
629         PT(i,13) = MassMR;
630         if PT(i,11) == 0
631             TNMR = TNMR + 1;
632         else
633             FPMR = FPMR + 1;
634         end
635     end
636     if PT(i,1) == 2 && P(i,12) == 3
637         LR = LR +1;
638         if PT(i,11) == 0
639             TNLR = TNLR + 1;
640         else
```

```
641                 FPLR = FPLR + 1;
642             end
643         end
644     end
645
646     FPrSR = FPSR/SR;
647     FPrMR = FPMR/MR;
648     FPrLR = FPLR/LR;
649
650     %Non-plastics
651
652     for i = 1:1:nT
653         if PT(i,1) == 3 && P(i,12) == 1
654             SW=SW+1;
655             PT(i,13) = MassSW;
656             if PT(i,11) == 0
657                 TPSW = TPSW + 1;
658             else
659                 FNSW = FNSW + 1;
660             end
661         end
662         if PT(i,1) == 3 && P(i,12) == 2
663             MW = MW + 1;
664             PT(i,13) = MassMW;
665             if PT(i,11) == 0
666                 TPMW = TPMW + 1;
667             else
668                 FNMW = FNMW + 1;
669             end
670         end
671         if PT(i,1) == 3 && P(i,12) == 3
672             LW = LW +1;
673             PT(i,13) = MassLW;
674             if PT(i,11) == 0
675                 TPLW = TPLW + 1;
676             else
677                 FNLW = FNLW + 1;
678             end
679         end
680     end
681
682     FNrSW = FNSW/SW;
683     FNrMW = FNMW/MW;
684     FNrLW = FNLW/LW;
685
686     SAP = 0;
687     SAW = 0;
688     TNSAP = 0;
689     FPSAP = 0;
690     TPSAW = 0;
```

```
691 FNSAW = 0;
692 %Stationary agglomeration
693 for i = 1:1:nT
694     if PT(i,1) == 4 || PT(i,1) == 6
695         SAP=SAP+1;
696         PT(i,13) = MassSAP;
697         if PT(i,11) == 0
698             TNSAP = TNSAP + 1;
699         else
700             FPSAP = FPSAP + 1;
701         end
702     end
703     if PT(i,1) == 5 || PT(i,1) == 7
704         SAW = SAW + 1;
705         PT(i,13) = MassSAW;
706         if PT(i,11) == 0
707             TPSAW = TPSAW + 1;
708         else
709             FNSAW = FNSAW + 1;
710         end
711     end
712 end
713
714
715
716 PT( ~any(PT,2), : ) = [];
717
718 MaterialClass = ["Small Foils";"Middle Foils";"Large Foils";"Small Rigids";"
        Middle Rigids";"Large Rigids";"Small N-P";"Middle N-P";"Large N-P"];
719 TotalInput = [SF;MF;LF;SR;MR;LR;SW;MW;LW];
720 FalseCallrate = [FPrSF;FPrMF;FPrLF;FPrSR;FPrMR;FPrLR;FNrSW;FNrMW;FNrLW];
721
722 Table = table(MaterialClass,TotalInput,FalseCallrate);
723
724 %% Results Mass
725
726 TNM = TNSF * MassSF + TNMF *MassMF + TNLF * MassLF + TNSR * MassSR + TNMR *
        MassMR + TNSAP *MassSAP;
727 FPM = FPSF * MassSF + FPMF *MassMF + FPLF * MassLF + FPSR * MassSR + FPMR *
        MassMR + FPSAP * MassSAP;
728
729 TPM = TPSW * MassSW + TPMW *MassMW + TPLW * MassLW + TPSAW * MassSAW;
730 FNM = FNSW * MassSW + FNMW *MassMW + FNLW * MassLW + FNSAW * MassSAW;
731
732 Grade = TNM / (TNM+FNM);
733 Massrecovery = (TNM + FNM) / (TNM+FNM+TPM+FPM);
734 Recovery = TNM / (TNM + FPM);
735
736
737 %% Monte Carlo results
```

```
738
739
740 Monte(j,1) = Grade;
741 Monte(j,2) = Recovery;
742 Monte(j,3) = Massrecovery;
743 Monte(j,4) = FPrSF;
744 Monte(j,5) = FPrMF;
745 Monte(j,6) = FPrLF;
746 Monte(j,7) = FPrSR;
747 Monte(j,8) = FPrMR;
748 Monte(j,9) = FNrSW;
749 Monte(j,10) = FNrMW;
750 Monte(j,11) = FNrLW;
751 Monte(j,12) = FP/(FP+TN);
752 Monte(j,13) = FN/(FN+TP);
753 Monte(j,14) = S_TypeError(1,4);
754 Monte(j,15) = S_TypeError(1,5);
755 Monte(j,16) = S_TypeError(1,6);
756 Monte(j,17) = S_TypeError(1,7);
757 Monte(j,18) = S_TypeError(1,8);
758 Monte(j,19) = S_TypeError(1,9);
759 Monte(j,20) = S_TypeError(1,10);
760
761 Stdev = nanstd(Monte);
762 Mean = nanmean(Monte);
763
764 Check = TP + TN + FP + FN;
765
766 Plastics= TN + FP;
767 NonPlastics = TP + FN;
768
769 NPINPUT = NonPlastics/Check;
770 end
771
772
773 %% Graphs and Tables
774
775 MaterialClass = ["Small Foils";"Middle Foils";"Large Foils";"Small Rigids";"
      Middle Rigids";"Large Rigids";"Small N-P";"Middle N-P";"Large N-P"];
776 TotalInput = [SF;MF;LF;SR;MR;LR;SW;MW;LW];
777 FalseCallrate = [FPrSF;FPrMF;FPrLF;FPrSR;FPrMR;FPrLR;FNrSW;FNrMW;FNrLW];
778 TypeofError = ["Systemic";"WR: Size";"WR: Classification"; "WR: Orientation";"
      Overlap";"St Agglomeration"; "Non-st Agglomeration"];
779
780 Values = ["Grade";"Recovery";"Mass Recovery";"FPr Small Foils";" FPrMiddle
      Foils";"FPr Large Foils";"FPr Small Rigids";"FPr Middle Rigids";"FNr Small
      N-P";"FNr Middle N-P";"FNr Large N-P"; "FPr Total"; "FNr Total" ];
781 MeanValues_Monte_Carlo  = Mean(1, 1:13)';
782 STDvalues_Monte_Carlo = Stdev(1,1:13)';
783
```

```
784 Table1 = table(MaterialClass,TotalInput,FalseCallrate);
785 Table2 = table(Values, MeanValues_Monte_Carlo,STDvalues_Monte_Carlo);
786
787 figure()
788 histogram(PT(:,11));
789 title('Number of errors per particle')
790 xlabel('Number of Errors')
791 ylabel('Number of particles')
792
793
794 X = categorical(TypeofError);
795 figure()
796 bar(X,Mean(1,14:20))
797 xlabel('Type of Errors')
798 ylabel('Number of particles')
799
800 %% Print
801
802 Table2
803
804 toc
805
806 % MassNP = 0;
807 % MassP = 0;
808 %
809 % for i = 1:1:nT
810 %     if PT(i,1) == 3 || PT(i,1) == 5
811 %         MassNP = MassNP + PT(i,13);
812 %     else
813 %         MassP = MassP + PT(i,13);
814 %     end
815 % end
816 %
```